Award Number: W81XWH-12-1-0366

TITLE: Integrated Immunotherapy for Breast Cancer

PRINCIPAL INVESTIGATOR: Peter P. Lee, MD

CONTRACTING ORGANIZATION: Beckman Research Institute of City of Hope
Duarte, CA 91010

REPORT DATE: September 2015

TYPE OF REPORT: Annual

PREPARED FOR: U.S. Army Medical Research and Materiel Command
Fort Detrick, Maryland 21702-5012

DISTRIBUTION STATEMENT: Approved for Public Release;
Distribution Unlimited

The views, opinions and/or findings contained in this report are those of the author(s) and should not be construed as an official Department of the Army position, policy or decision unless so designated by other documentation.

REPORT DOCUMENTATION PAGE

Form Approved
OMB No. 0704-0188

Public reporting burden for this collection of information is estimated to average 1 hour per response, including the time for reviewing instructions, searching existing data sources, gathering and maintaining the data needed, and completing and reviewing this collection of information. Send comments regarding this burden estimate or any other aspect of this collection of information, including suggestions for reducing this burden to Department of Defense, Washington Headquarters Services, Directorate for Information Operations and Reports (0704-0188), 1215 Jefferson Davis Highway, Suite 1204, Arlington, VA 22202-4302. Respondents should be aware that notwithstanding any other provision of law, no person shall be subject to any penalty for failing to comply with a collection of information if it does not display a currently valid OMB control number. **PLEASE DO NOT RETURN YOUR FORM TO THE ABOVE ADDRESS.**

1. REPORT DATE	2. REPORT TYPE	3. DATES COVERED
September 2015	Annual	1Sep2014 - 31Aug2015

4. TITLE AND SUBTITLE
Integrated Immunotherapy for Breast Cancer

5a. CONTRACT NUMBER

5b. GRANT NUMBER
W81XWH-12-1-0366

5c. PROGRAM ELEMENT NUMBER

6. AUTHOR(S)

Peter P. Lee, MD

E-Mail: plee@coh.org

5d. PROJECT NUMBER

5e. TASK NUMBER

5f. WORK UNIT NUMBER

7. PERFORMING ORGANIZATION NAME(S) AND ADDRESS(ES)

Beckman Research Institute of City of Hope
Duarte, CA 91010

8. PERFORMING ORGANIZATION REPORT NUMBER

9. SPONSORING / MONITORING AGENCY NAME(S) AND ADDRESS(ES)
U.S. Army Medical Research and Materiel Command
Fort Detrick, Maryland 21702-5012

10. SPONSOR/MONITOR'S ACRONYM(S)

11. SPONSOR/MONITOR'S REPORT NUMBER(S)

12. DISTRIBUTION / AVAILABILITY STATEMENT
Approved for Public Release; Distribution Unlimited

13. SUPPLEMENTARY NOTES

14. ABSTRACT
Over the last 12 months of this award, we have focused on developing an in-depth understanding of the immune system in the setting of the tumor microenvironment. We have made progress in developing methods to better analyze the relationships between primary tumor and metastatic growths with their surrounding microenvironments, and implications for immune response and dendritic cell function *in vitro* using 3D microculture techniques. We have further investigated and tested alternative methods for tumor eradication using combinatorial drugs in attempts to restore/enhance the immune response. Additionally, we continue preparing breast cancer cell lines to aid quantifying progress in *in vivo* studies using mouse models. We anticipate that the progress made in these last 12 months will lead to combining observations into *in vitro* and *in vivo* models to better test our combinatorial immunotherapeutic strategies, restore dendritic cell function in cancer, and identifying novel tumor-associated stroma targets.

15. SUBJECT TERMS
Breast Cancer, immunotherapy, tumor microenvironment, dendritic cells, metastasis, cancer stroma.

16. SECURITY CLASSIFICATION OF:			17. LIMITATION OF ABSTRACT	18. NUMBER OF PAGES	19a. NAME OF RESPONSIBLE PERSON
a. REPORT	b. ABSTRACT	c. THIS PAGE			USAMRMC
U	U	U	UU	41	19b. TELEPHONE NUMBER *(include area code)*

Table of Contents

Page

Introduction…….……..…….. 4

Body…….…….. 5

Results Aim 1 ……..……. 5

Results Aim 2 ……15

Results Aim 3 ……22

Key Research Accomplishments…….……..37

Reportable Outcomes……..……38

Conclusion……..38

Appendices……..……..38

Personnel……...…….38

References……..39

INTRODUCTION:

The immune system and cancer are both complex biological systems that interact and affect each other. While there have been recent successes in cancer immunotherapy including PROVENGE, a dendritic cell based vaccine for prostate cancer, and antibodies blocking immune checkpoints (CTLA-4 and PD-1) for melanoma, these have produced clinical benefits only in a subset of patients. The intimate relationships between cancer cells, immune cells, and tumor associated stromal cells must be explored and investigated in order to truly have an effective immunotherapy for breast cancer. It has more recently become clear that not only does the immune system respond to cancer cells, but the process goes both ways, with cancer also able to suppress the host immune system. Tumor-infiltrating lymphocytes (TILs) have been shown to be functionally impaired in many cancers (*1*). In tumors where TILs were found to be functional, the prognosis was consistently favorable (*2, 3*). The collective data suggest that T cell infiltration—when functionally active—leads to a favorable outcome in breast cancer. These data concerning the tumor environment complement our own findings that changes in immune cells within tumor-draining lymph nodes (TDLNs) strongly correlate with clinical outcome in breast cancer (*4*). Despite the complexity, certain elements can be teased out and focused upon for maximal impact. Our previous studies have led to key insights into the mechanisms behind the immune dysfunction that breast cancer causes. Comprehending how the different phases—activation, expansion and effector functions—of a normally functioning immune response are disrupted in the presence of breast cancer will allow us to develop strategies to counteract the problems and restore immune function to optimal levels in patients. This focus on unraveling the dynamics between breast cancer and host immune system in a comprehensive and systematic manner is the underlying principle of my goal to develop rational combination immunotherapy for breast cancer, one that is truly effective long term at eliminating metastases and thereby preventing relapse in breast cancer patients. In order to build on the observations my lab has made with regards to cancer-dendritic cell function and immune cell-cancer relationships, immune responses within the tumor microenvironment must be analyzed in depth to identify unique markers, molecular and cytokine signals, and associated cell populations which may be aiding in immunosuppression. To this end, I have built a strong research team for this project, which includes assistant research professor Dr. Brile Chung, PhD postdoctoral fellow Dr. Dobrin Draganov, research associates Gayathri Srinivasan and Gilbert Acosta. We worked closely with clinical collaborators at the City of Hope under an IRB approved protocol. In this annual report, I will discuss the foundation being laid toward the goals outlined in our statement of work, and the approaches that we will test to remedy the global immune dysfunction in breast cancer.

BODY:

We have a strong research team for this project, which includes assistant research professor Dr. Brile Chung, PhD postdoctoral fellow Dr. Dobrin Draganov, research associates Gayathri Srinivasan and Gilbert Acosta. We worked closely with the CoH IRB office on a human subject's protocol which has been approved. We have close collaborations with breast cancer surgeons, pathologists, and the tissue bank at CoH in order to procure breast cancer tissue, lymph node, and blood samples for our analyses. Animal work has begun under two animal protocols (IUCAC #13042 and #04040) which have been approved at City of Hope and the DoD. Our team established cell lines, protocols, *in vitro* and *in vivo* experiments to facilitate tasks in our statement of work. Listed below are the main aims which we proposed, corresponding tasks from our statement of work, and our progress to-date.

Aim 1. Enhance efficacy of dendritic cell (DC)-based vaccination by promoting DC maturation and clustering in vivo.

Task 1. Identifying mechanisms by which breast cancer disrupts DC clustering and maturation : months 1-48.

Task 2. Testing novel strategies to enhance DC clustering *in vivo*: months 1-48.

Aim 2. Enhance T cell function *in vivo* by restoring immune signaling.

Task 3. Investigating mechanisms by which chronic IL6 affects immune function: months 1-36.

Task 4. Testing the effectiveness of IL6-blockade plus IL27 treatment in reversing chronic IL6-induced T cell dysfunction: months 12-48.

Aim 3. Select optimal integrated immunotherapy combinations in animals for clinical development.

Task 5. Select Optimal Integrated Immunotherapy Combinations in Animal Models for Clinical Development: months 12-60.

Results:

<u>Aim 1. Enhance efficacy of dendritic cell (DC)-based vaccination by promoting DC maturation and clustering *in vivo.*</u>

Task 1. Identifying mechanisms by which breast cancer disrupts DC clustering and maturation: months 1-48.

a. Test effects of known breast cancer secreted molecules on DC clustering and maturation (month 1-36).

b. Identify novel breast cancer secreted molecules on DC clustering and maturation using proteomics and gene expression analysis after laser capture micro-dissection (month 1-48).

In order to gain knowledge on the molecules and factors which influence DC clustering and maturation, especially in the context of cancer, we first need to establish a better understanding of the dynamics between immune cells and the tumor microenvironment. To this end, we have worked to establish an *in vitro/ex vivo* model which helps mimic cell-cell interactions in a 3D microenvironment. It has been established in recent years that 3D cell culture environments provide a more physiological representation of cell interactions. 3D cultures also produce markers and behavior that might not be seen on traditional monolayer culture experiments, and applies also specifically to the breast cancer setting (5). The tumor microenvironment is comprised of heterogeneous populations of cells including cancer, immune, and cancer-associated stromal cells

(CAS) to name a few. Clinical data and experimental models have shown that the extent and nature of immune infiltrations into tumors is an important independent prognostic factor (*6*). Recent findings suggest that CAS is another important regulator of tumor growth and progression which may also modulate the recruitment, activation status, and retention of immune cells in the tumor microenvironment (*7*). Therefore, targeting the CAS plus cancer cells is essential for the success of cancer immunotherapy.

Progression of tumor growth and initiation of metastasis is critically dependent on the reciprocal interactions between cancer cells and tumor associated stroma. CAS have been known to promote inhibitory effect on T cells by producing various factors and cytokines such as TGF beta, VEGF, HGF, IL-6, and IL-17 (*8*). These factors also may play a very important role in understanding the characteristics of DC's in the tumor microenvironment. Here, we have developed 3D cell aggregate culture system that recapitulates the human tumor microenvironment by incorporating essential populations of CAS to investigate the dynamic relationship between the tumor microenvironment and the immune system. Our novel approach focuses on separate expansion and later re-aggregation of the subpopulations of primary human breast cancer stroma and immune cells that are critical for supporting or inhibiting cancer growth. A major advantage of our tumor aggregate system is that cancer, stromal, and immune cells can be easily manipulated *in vitro*, i.e. cell numbers, mixture of ratios, etc. (**Figure 1**). Furthermore, we are performing genomic profiling of cancer cells and CAS to identify differential gene expression patterns in these reconstructed co-cultured cancer cell/stromal cell 3D organoids (**Figure 2**).

The role of mesenchymal stem cells in cancer

Bone marrow-derived mesenchymal stem cells (MSC) have been the subject of interest in solid tumor. Because of their ability to migrate to sites of inflammation and tissue repair, the studies have shown that MSC can also be recruited to various solid tumor microenvironments and promote cancer cell survival, proliferation, and differentiation (*9, 10*). In addition, high levels of various cancer-associated factors, including TGF-β and chemokine ligand 16 (CXCL16) in the tumor microenvironment can convert the newly recruited MSCs into cancer-associated fibroblasts (CAFs), which further promote progression of metastasis. We conducted a pilot study where we expanded C57 B6 derived bone marrow MSCs and characterized them using flow cytometry (**Figure 3**). These cells expressed the common MSC markers, i.e. CD44, CD140β, and CD105 and were negative for CD45 and were stably transduced B6-derived E007 breast cancer cells with the retroviral vector containing both Luciferase and GFP cDNA (**Figure 4**). A schematic diagram of the in vivo study is shown in **Figure 5**. Briefly, E007 cells alone or in combination with MSCs were injected into the mammary fat pad and tumor engraftment was assessed 10 days later (**Figure 6**). This pilot study demonstrated that the injection of suspended E007 in C57BL/6 mouse created tumors from injection into the mammary fat pad.

Instead of injecting suspended E007 cancer cell line that was transduced with the IRES retroviral containing luciferase and GFP cDNA, we next seek to insert a 3-D cell aggregate that was created ex vivo under the skin of a C57BL/6 recipient animals. Following engraftment, one of the implanted 3-D cell aggregates will be subcutaneously cryo-ablated in order to stimulate langerhan dendritic cells and other antigen presenting cells (APCs) that reside in the skin and allow these APCs to migrate to nearby lymph nodes for T cell activation. The purpose of this site-specific cryo-ablation is to: 1) induce E007 cell death and, 2) allow E007 associated cancer antigens to be picked up by APCs located in the area nearby cryo-ablation. If successful immune activation is achieved by subcutaneous ablation, we will investigate whether activated T cells can efficiently eradicate other subcutaneously implanted aggregates. This will provide a novel technique to achieve successful cancer cell immunization.

Being able to insert a cell aggregate into the mammary fat pad of the mouse will allow us to more realistically recapitulate the development and niche of the tumor microenvironment. Although a previous pilot experiment involving the injection of suspended E007 in C57BL/6 mouse proved that we can successfully create tumors from injection in the mammary fat pad, we believe that a cell aggregate inserted in the same region will allow for a slower and more easily distinguishable tumor progression. In addition, naturally developing breast tumors are composed of both cancer cells and mesenchyme-derived stromal cells in their

tumor microenvironment. Stromal cells in the tumor microenvironment are extremely critical for protection, proliferation, mutation, and differentiation of cancer cells. It is well known that implanted E007 tumor cells (via injection) do not recruit host-derived stromal cells efficiently.

Utilizing human breast tumor tissues, we have previously shown that breast cancer associated fibroblasts (CAFs) can be isolated, expanded (*ex-vivo*), and re-aggregated into a functional three-dimensional tumor microenvironment. To investigate whether CD44+ CAF adherent cells express mesenchyme-derived surface markers, we analyzed immuno-phenotypic characterization of the monolayer generated in breast tumor fragment cultures after 3 weeks by FACS. Almost all the ex-vivo expanded mesoderm-derived fibroblasts from normal breast and CAFs from primary and brain-met tissues expressed the common mesenchyme markers, CD44, CD90, CD105, CD166, and CD140β (**Figure 7A**). Moreover, quantitative RT-PCR analysis demonstrated that EGF, FGF, and IGF, important factors known to support the growth of cancer cells, are expressed by CAFs (**Figure 7B**), providing evidence that cultured CAFs produce factors important for maintenance of patient-specific breast cancer cells. In order to demonstrate the ability of 3-D aggregates to produce and maintain important extra-cellular matrix (ECM) and maintain CAF markers, the cell aggregates were cultured for 2 weeks and paraffin-sectioned for IHC analyses. Histologic analysis of the paraffin aggregates illustrated that important ECM such as collagen IV and fibronectin are conserved in all the aggregates when compared to breast tumor tissues (**Figure 8**). The presence of fibroblastic activating protein (FAP) and alpha smooth muscle actin (α-SMA) has been well described in myofibroblasts and CAF. As expected, both FAP and α-SMA expressing cells were more prevalent in the primary and brain met aggregates when compared to the normal aggregates. Based on our findings, we further generated 3-D CAF aggregates mixed with human breast cancer cells in order to recapitulate human breast tumor tissue microenvironment (**Figure 9**). This technique will be further utilized for implantation of mouse-based 3-D E007+MSC aggregate into B6 tumor recipient animals.

Breast cancer secreted molecules on DC clustering and maturation using proteomics and gene expression analysis

In order to better evaluate the molecules or factors that may be affecting DC clustering and maturation, we must be able to re-create a suitable method for recapitulating the tumor microenvironment in a controlled setting. The 3D culturing techniques presented and used identify a more physiological method (versus monoculture *in vitro*) for identifying the interactions between tumor microenvironment and immune cells. The method of using 3D aggregate cultures will allow us to create an isolated environment of PBMC derived DCs along with tumor associated stroma or healthy stroma cells, and with or without primary tumor involvement if desired. The cells then can be analyzed via histological analysis, as demonstrated previously, from paraffin embedded 3D aggregate cultures to identify DC populations. Laser capture microdissection can then be utilized on these 3D aggregate sections and run for analysis of genetic expression changes of the DCs exposed to tumor associated stroma versus healthy stroma. Futhermore, results can be compared to genetic expression microarray profiles available in public domain. Specifically, utilizing a deconvolution methodology, which was developed by our lab (*11*), we are able to perform analysis of cell-type specific gene expression using existing large pools of publically available microarray datasets and identify if the trends found in our 3D aggregate analysis for DC populations is identified in other tumors/cancers (*11*). We also have begun banking tumor associated stromal RNA, healthy stromal RNA, as well as tumor RNA for future analysis on microarray or RNAseq to identify unique markers which may be influencing DC clustering or maturation as well as other potential implications to surrounding immune cells in the tumor microenvironment.

Task 2. Testing novel strategies to enhance DC clustering *in vivo*: months 1-48.

a. Test agents known to modulate DC clustering and maturation in vitro (month 1-24).

b. Test molecules that block factors identified in task 1 (month 12-48).

The maturation status of dendritic cells (DCs) plays an important role in determining the nature of an immunologic response. Mature DCs are capable of eliciting an effective "immunogenic" response. An effective anti-tumor response is elicited when DCs present tumor antigens to T cells leading to activation and proliferation of specific T cells. Over the past decade, there has been considerable effort made to characterize DC populations in cancer. A pivotal location to examine such immune-tumor interactions is the tumor-draining lymph node (TDLN). It is the site where tumor antigens are typically first presented to the immune system and a critical initial decision between immune activation and tolerance is made. We have previously shown that DCs in healthy lymph nodes (HLNs) tend to aggregate in large clusters of mature cells, whereas DCs in TDLNs tend to remain either un-clustered or form smaller clusters with fewer mature cells. This clustering behavior promotes functionality of DCs by increasing the number of proximal T cells compared to un-clustered DCs. Intriguingly, the degree of DC clustering within TDLNs correlated strongly with better clinical outcome in breast cancer patients. Further progress and results from Task 1 will inform design of experiments in this Task.

Plans for the next 12 months:

- Create an *ex vivo* 3-D cell aggregate containing E007 cancer cells and MSCs derived from C57BL/6 bone marrow and implanting the 3-D aggregates under the skin of C57BL/6 mice and assess engraftment. Following engraftment, one of the aggregates will be cryo-ablated to stimulate APCs and T cell activation and cytotoxicity will be assessed.

- Attempt to identify potential markers on stromal cells or cancer cells which may be producing unique immunosuppressive properties.

- Perform analysis on tumor associated and healthy stroma in the tumor microenvironment by microarray or RNAseq to help identify unique genetic expression profiles or functional defects which may influence tumor progression/metastasis.

- Monitor effect of modulation of DC clustering/maturation by testing known agents previously investigated and mentioned above, by utilizing assays in 3D aggregate cultures and 3D hydrogel matrix systems.

Supporting Data/Figures:

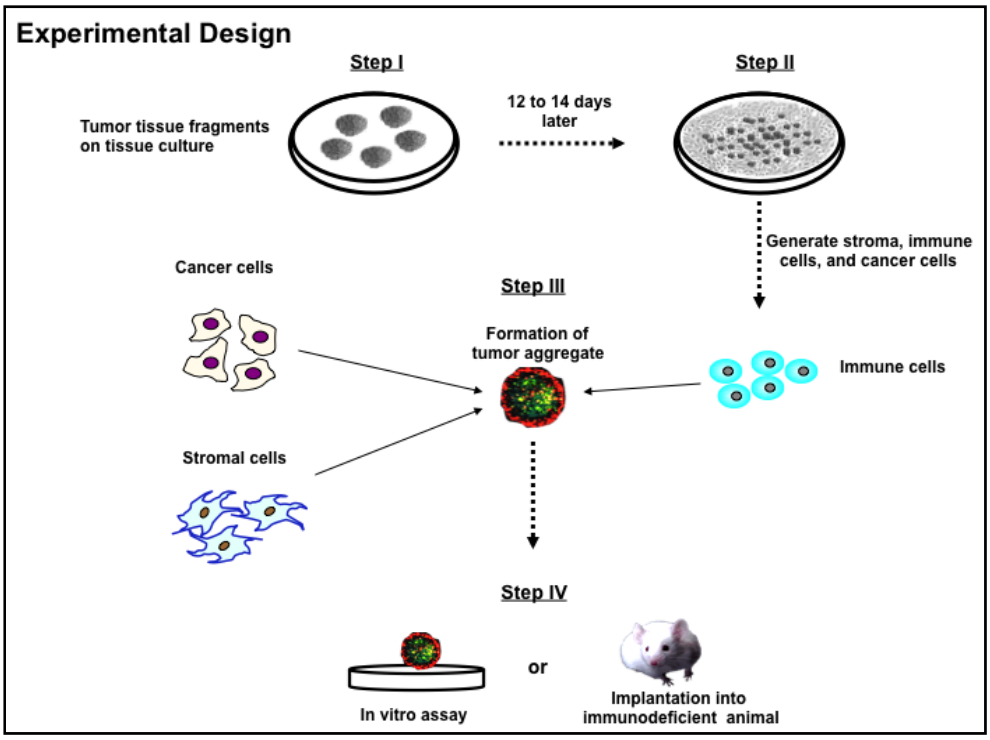

Figure 1- Experimental Design**.** Illustration of the steps involved in producing 3D aggregate populations from tumor associated cells and use *in vitro* or potentially *in vivo.*

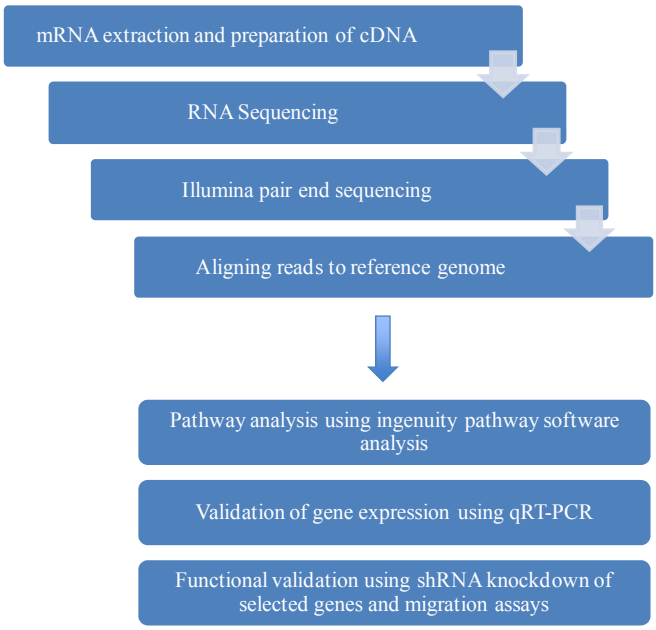

Figure 2: Experimental Design**.** Illustration of the steps involved in genomic profiling of cancer cells and CAS to identify differential gene expression patterns in the reconstructed co-cultured cancer cell and stromal cell 3D organoids.

.

Phenotypic characterization of Murine bone marrow-derived MSC

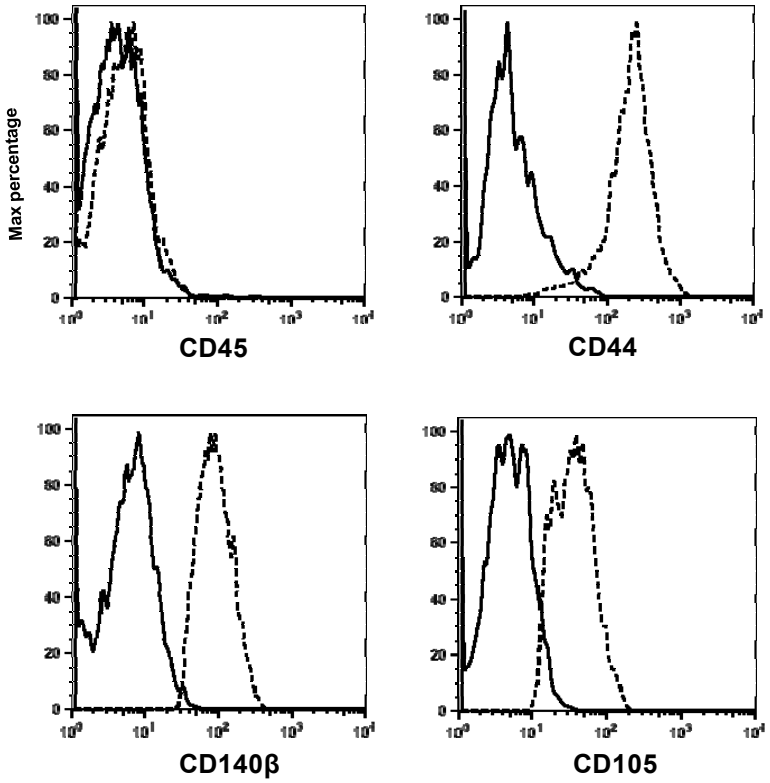

Figure 3. Characterization of ex-vivo expanded C57 B6 derived bone marrow mesenchymal stem cells. The cells are positive for CD44, CD140β, CD105, and negative for CD45.

Transduction of B6-derived E007 breast cancer cell line

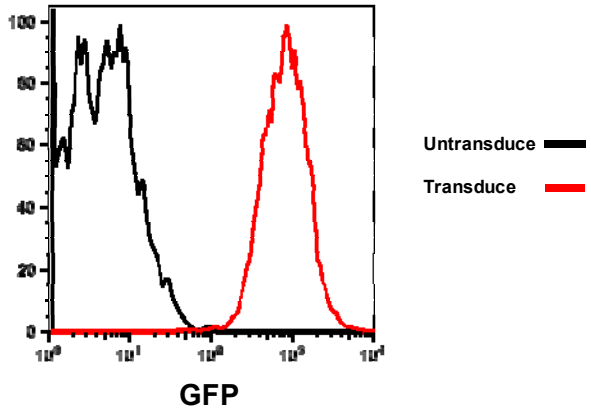

Figure 4. Stably transduced B6-derived E007 breast carcinoma with the retroviral vector containing both Luciferase and GFP cDNA. Post-transduction, FACS Aria Automated Cell Deposition Unit (ACDU) was performed.

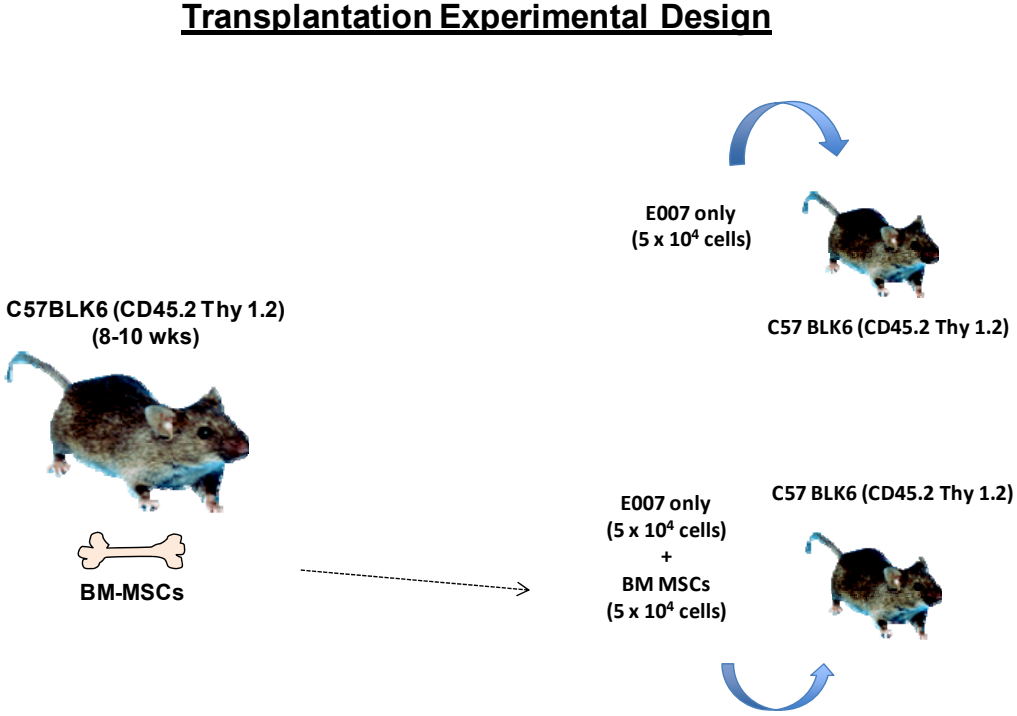

Figure 5. Schematic diagram of *in vivo* study. *Ex-vivo* expanded BM-derived MSCs were co-transplanted with E007 mouse breast cancer cell line.

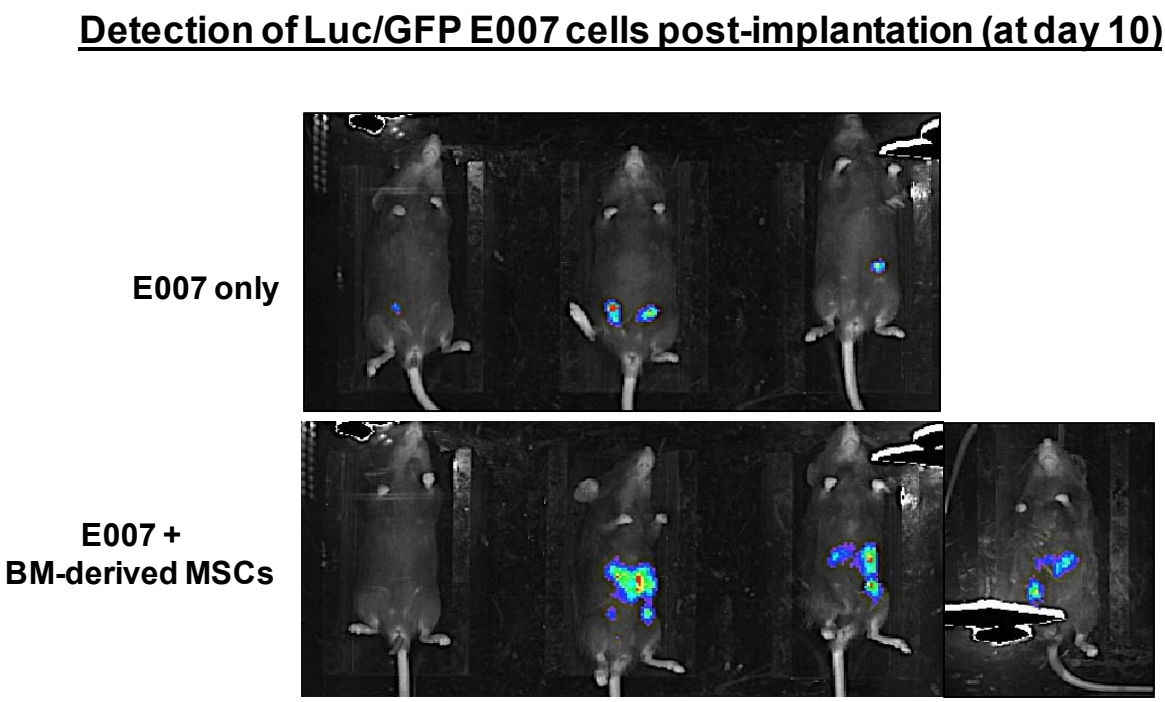

Figure 6. Imaging of E007 engraftment (with or without co-transplantation of MSCs). Images are of representative mice that received transplants of luciferase-expressing E007 cells. All successive images in each row were taken from the same recipients after transplantation at days shown.

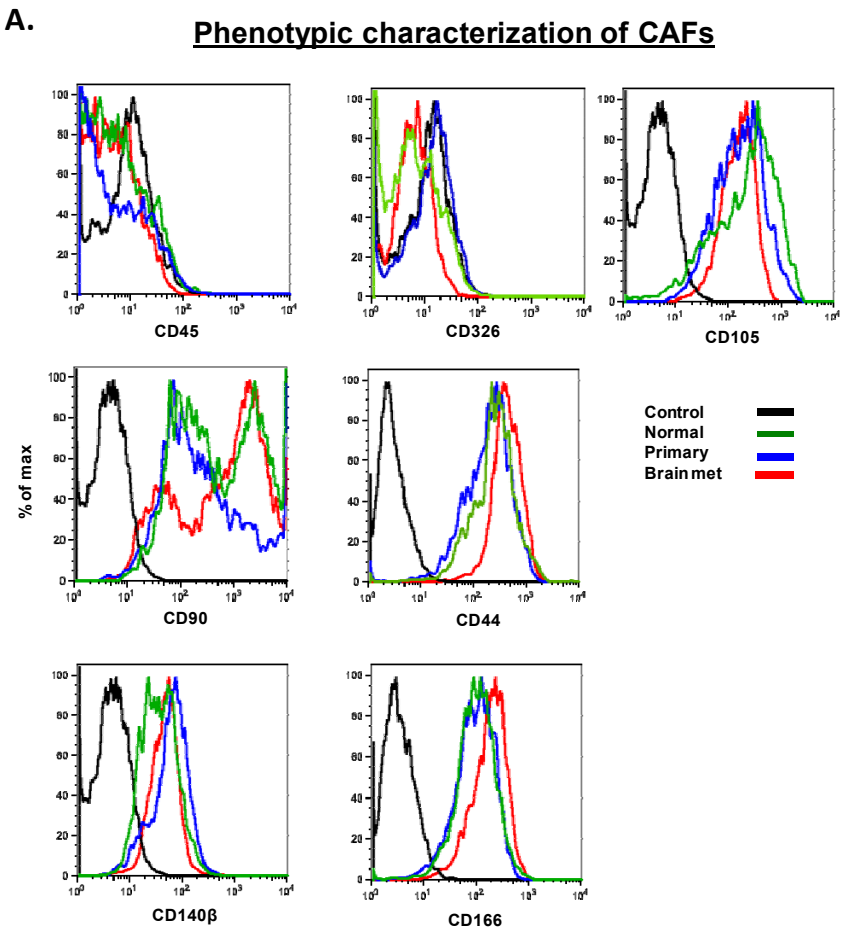

Figure 7. Characterization of cancer associated fibroblasts (CAFs). A). Ex-vivo expanded mesoderm-derived fibroblasts from normal breast and CAFs from primary and brain-met tissues expressing common mesenchyme markers, CD105, CD166, CD90, CD44, CD140β, CD105, and negative for CD45 and CD326. B). qRT-PCR analysis demonstrating that EGF, FGF, and IGF are expressed by CAFs.

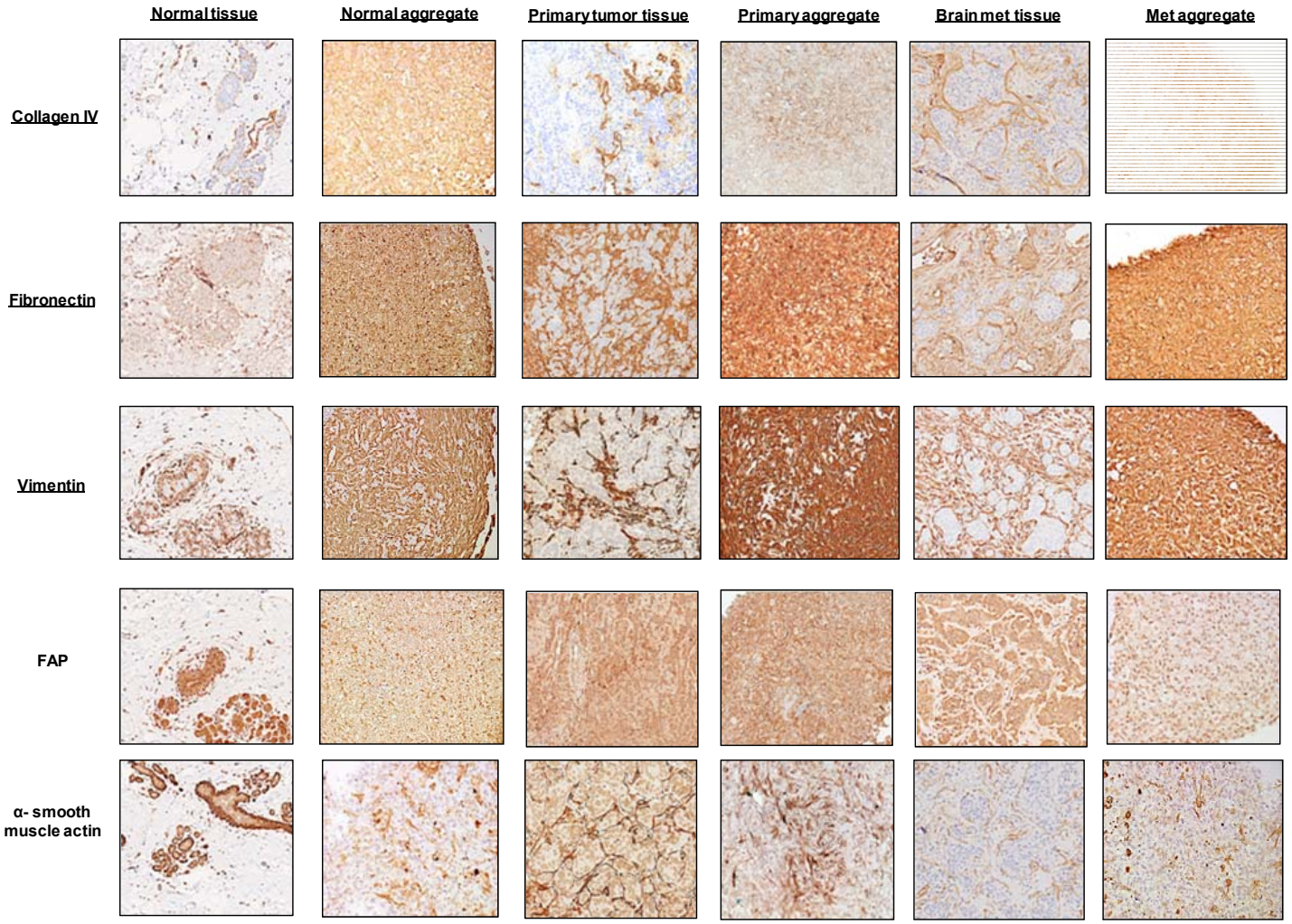

Figure 8. Histologic analysis of normal, primary breast tumor, and metastatic tissue and corresponding 3-D aggregates. Cell aggregates were cultured for 2 weeks and paraffin-sectioned for IHC analysis. Tissue sections or cell aggregate sections were stained for collagen IV, fibronectin, vimentin, fibroblastic activating protein (FAP), and α-smooth muscle actin and chromogen was developed by DAB (brown). Tissues were counter stained with hematoxylin (200x magnification).

Con-focal image of 3-D aggregate (CAF+ breast cancer cells)

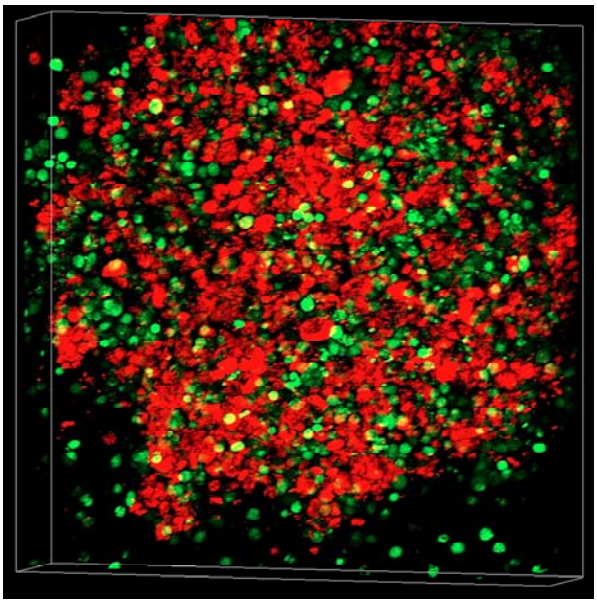

CAFs: Red
Cancer: Green

Figure 9. Con-focal Z-stack imaging of 3-D aggregates

Aim 2. Enhance T cell function *in vivo* by restoring immune signaling.

Task 3. Investigating mechanisms by which chronic IL-6 affects immune function: months 1-36.

a. Gene expression analyses and flow cytometry to measure expression of positive and negative signaling regulators (month 1-36).

b. T cell polarization and functional assays (month 1-36).

Task 4. Testing the effectiveness of IL-6-blockade plus IL-27 treatment in reversing chronic IL-6-induced T cell dysfunction: months 12-48.

a. In vitro assays to test the effects of treatment with an anti-IL-6 antibody plus IL-27 during naive CD4 T cell polarization and CD8+ T cell activation (month 12-36).

b. Test various treatment strategies to reverse T cell dysfunction in BC patients (month 24-48).

Multiple immune defects have been documented in cancer patients, which limit the ability of the host immune response to control cancer progression and metastases to prevent relapse. In addition, tumor-promoting immune functions have been shown to be up-regulated in cancer patients. The universal dysfunction of the immune system could be explained by a breakdown in communication via cytokines. IL-6 is a cytokine that signals through a receptor complex of GP130 and IL-6Ra to activate the STAT3 and STAT1 transcription factors (*12*). IL-6 has pleiotropic roles in disease and immune responses with a well-known role in promoting tumorigenesis. In cancer settings, IL-6 is produced by tumor cells, tumor stroma and tumor-associated myeloid cells and activates phosphorylation of STAT3 (pSTAT3) in tumor cells to promote survival and proliferation. STAT3 itself is considered an oncogene and also promotes the renewal of cancer stem cells (*13*).

Breast cancer patients are known to have elevated serum levels of IL-6, and higher serum IL-6 levels are associated with poorer survival in metastatic breast cancer patients (*14, 15*). Because of the strongly supported role of IL-6 in promoting tumorigenesis, multiple efforts are underway to inhibit IL-6 as a therapeutic intervention. For immune cells, IL-6 has vital roles in T cell activation, for instance by inhibiting T_{REG} while promoting T_H17 differentiation (*16*). Mice lacking IL-6 are unable to elicit effective immune responses against viruses and bacteria (*17, 18*). T cells from breast cancer patients are known to have impaired effector functions and are skewed towards T_{REG} populations. However the role of IL-6 in breast cancer patient T cell function has not been previously addressed. IL-27 also signals through GP130 paired with a unique receptor WSX-1 to activate STAT1 and STAT3 (*19*). IL-27 is known to enhance T_H1 and inhibit T_H2 polarization by synergizing with IL12 to promote IFNγ production and inhibiting T_H2 cytokine production (*20-22*). IL-27 was also shown to induce generation of effector CTLs from naive $CD8^+$ T cells in a STAT1-dependant manner (*23, 24*). Interestingly, IL-27 has anti-tumor activities *in vivo* in mice (*25*).

While both IL-6 and IL-27 activate STAT1 and STAT3, IL-6 tends to favor STAT3 activation, and IL-27 favors STAT1. STAT1 and STAT3 cross-regulate one another by competing for binding sites on cytokine receptors, upregulating expression of negative regulators, and can form heterodimers to alter promoter binding specificities (*26*). STAT1 and STAT3 mediate opposing effects on both tumor cell survival and immune cell activity. In tumor cells, STAT3 promotes survival and proliferation. In contrast, STAT1 promotes cell cycle arrest and apoptosis (*26*). In immune cells, cytokines, including IL-10 and VEGF, activate STAT3-mediated immune suppression, while STAT1 activation promotes antigen presentation, inflammatory responses, and T_H1 immunity (*26*). Immune cells lacking STAT3 exhibit enhanced tumor immune-surveillance (*27, 28*). These studies indicate the crucial balance of cytokine signaling in directing anti-tumor immune responses.

Evaluation of T cell responses to IL-6 in an expanded cohort of breast cancer patients.

Clinical and pathological characteristics of the BC patients studied are summarized in **Table 1**. Peripheral blood mononuclear cells (PBMCs) were obtained from BC patients or healthy donors and stimulated with IL-6 at 100ng/ml for 15mins. Phosphorylation of STAT1 and STAT3 (pSTATs) in $CD4^+$ naïve T cells ($CD3^+CD4^+CD45RA^+$) were determined by phosphoflow cytometry with anti-pSTAT1(pY701) and anti-pSTAT3(pY705) antibodies (*29*). IL-6 signaling responses (ΔMFI), represented by IL-6 stimulated minus

unstimulated pSTATs median fluorescence intensity (MFI), was compared between BC patients and age-matched healthy donors (**Figure 10A**). We found that IL-6 induced phosphorylation of STAT1 (p=0.001) and STAT3 (p<0.0001) in $CD4^+$ naïve T cells from BC patients (n=57, median age 51, range 27-85) were significantly lower than healthy donors (n=28, median age 53, range 18-72) (**Figure 10B**). In cancer cells, STAT1 and STAT3 are known to play opposite roles in tumorigenesis (*30*). Nevertheless, we found that the IL-6 induced phosphorylation of STAT1 and STAT3 are highly correlated (**Figure 10C**), indicating that IL-6 simultaneously activates both STAT1 and STAT3 pathways in $CD4^+$ naïve T cells.

Cytokine IL-6 plasma levels in breast cancer patients at diagnosis

IL-6 plasma levels have been shown to be elevated in advanced metastatic BC patients (*15, 31*). To investigate whether the observed impaired IL-6 signaling response in BC patients $CD4^+$ naïve T cells is caused by elevated IL-6 plasma levels, we compared the IL-6 plasma levels between BC patients (n=70, median age 50, range 27-85) and age-matched healthy donors (n=66, median age 58, range 18-72) by ELISA. All the plasma from BC patients was collected at diagnosis prior to surgery or any therapy. Interestingly, we found that IL-6 plasma levels were not significantly elevated in these BC patients (mean 4.2pg/ml, median 0pg/ml) compared to healthy donors (mean 2.0pg/ml, median 0.25pg/ml) (**Figure 11A**). We stratified IL-6 plasma levels into 3 categories consisting of the normal range (0-2 pg/ml), moderately above normal (2-10 pg/ml), and high (>10pg/ml) and found that the distribution of IL-6 levels were similar between BC patients and healthy donors (**Figure 11B**). Since normal IL-6 plasma levels are generally in the range of 0-2 pg/ml (*32*), these results suggest that most of the BC patients (74.3%) at diagnosis have normal IL-6 plasma levels. Furthermore, we compared the IL-6 signaling response between BC patients and healthy donors who have normal IL-6 plasma levels (0-2pg/ml) and found that IL-6 induced phosphorylation of STAT1 (p=0.04) and STAT3 (p=0.008) of $CD4^+$ naïve T cells from BC patients were significantly lower than that of healthy donors (**Figure 11C**). Moreover, we found no significant correlation between IL-6 plasma levels and IL-6 induced phosphorylation of STAT1 and STAT3 (**Figure 11D**) suggesting IL-6 plasma levels is not contributing to the observed IL-6 signaling defects in BC patients $CD4^+$ naïve T cells.

Identifying significant correlations between cytokine signaling response in immune cells and clinical outcome of breast cancer patients.

Breast cancer (BC) is a heterogeneous disease with varied presentation, morphology and clinical behavior. Currently, the risk of BC progression is evaluated based on numerous clinical and pathologic parameters include tumor size, histological grade, lymph node status, hormone receptor and HER2 status (*33*). However, most of these characteristics of tumor tissues can only be obtained after biopsy or surgery and have limited predictive power. As a result, a major challenge is the development of a prognostic blood test for BC patients at diagnosis prior to surgery.

To evaluate the prognostic potential of IL-6 signaling responsiveness, we compared the IL-6 induced phosphorylation of STAT1 and STAT3 in peripheral $CD4^+$ native T cells between relapsed and non-relapsed BC patients. The patient selection criteria for this analysis was: 1) Patients with blood collected at diagnosis prior to surgery or any therapy and, 2) Patients have been clinically followed for at least 36 months. The median follow-up time of BC patients (n=40) was 63 months (range 17-92 months). We found that IL-6 induced phosphorylation of STAT1 (p=0.0003) and STAT3 (p=0.0001) were significantly lower in relapsed than in non-relapsed BC patients (**Figure 12A**). Survival analysis was performed to evaluate the correlation between IL-6 signaling response and relapsed-free survival (RFS). To impartially stratify BC patients (n=40) into two populations, the median ΔMFI of IL-6 induced pSTAT1 (median 91 ΔMFI) or pSTAT3 (median 387 ΔMFI) was used. Interestingly, we found that BC patients with pSTAT1 (p=0.004) or pSTAT3 (p=0.005) ΔMFI below the median (n=20) had significantly worse RFS than those above the median ΔMFI (n=20) (**Figure 12B**), and that lower IL-6 signaling responses predicted worse RFS. In addition, all the relapsed patients had IL-6 signaling responses below the median value while all of the non-relapsed patients had IL-6 signaling response above the median value (**Figure 12B**). Among the relapsed BC patients, we compared the IL-6 signaling

response between patients with blood collected at diagnosis (n=7) and patients with blood collected at relapsed (n=7) and found no significantly difference of IL-6 induced phosphorylation of STAT1 and STAT3 between these two time points (**Figure 13**), suggesting that the impaired IL-6 signaling responses are prolonged during BC progression. Importantly, in a multivariate analysis adjusting for age, tumor stage, grade, nodal status and subtype, IL-6 induced phosphorylation of STAT1 (p=0.001) or STAT3 (p=0.005) still retained the prognostic significance for RFS, indicating that IL-6 signaling responses could be a predictor for clinical outcome independent of these clinicopathologic characteristics (**Table 2**). The associations between IL-6 signaling response and clinicopathologic characteristics of BC patients were also evaluated and no significant correlation was found between IL-6 signaling response and age, tumor stage, grade, T status or subtype of BC patients (**Table 3**). Therefore, these findings suggest that IL-6 signaling responsiveness in peripheral $CD4^+$ naïve T cells potentially could be developed into a prognostic blood test given at diagnosis to predict the clinical outcome of BC patients.

Plans for the next 12 months:

- Determine the functional consequences caused by impaired cytokine signaling response in immune cells, e.g. T cell proliferation, Treg/Th17 differentiation.

- Investigate whether signaling responses of other cytokines, such as IL-27, IFNγ, IL-10 and TGFβ, potentially predict clinical outcome of breast cancer.

Supporting Data/Figures:

Table I Patients characteristics

Characteristics	Patients (N=77)
Age—yr	
Median	50
Range	27-85
Tumor stage— no.(%)	
DCIS	8 (10.4)
T1	31 (40.2)
T2	25 (32.5)
T3	9 (11.7)
Unknown	4 (5.2)
Grade— no.(%)	
G1	9 (11.7)
G2	33 (42.8)
G3	35 (45.5)
Nodal status— no.(%)	
N0	42 (54.5)
N1-3	31 (40.3)
Unknown	4 (5.2)
Subtype— no.(%)	
Luminal	64 (83.1)
HER2	6 (7.8)
Triple negative	7 (9.1)

Table 2. Univariate and multivariate analysis for relapse-free survival by Cox regression

Variables	Univariate	Multivariate
	p-value	p-value*
pSTAT1	0.006	0.001
pSTAT3	0.015	0.005

Note: *adjusting for age, tumor stage, grade, nodal status and subtype

.

Table 3 Correlation between IL-6 signaling response and clinicopathological characteristics

Variables	pSTAT1	pSTAT3
	r (p-value)	r (p-value)
Age	0.13 (0.34)	0.05 (0.72)
Tumor stage	-0.13 (0.38)	-0.01 (0.99)
Grade	-0.03 (0.82)	0.1 (0.45)
Nodal status	-0.02 (0.89)	0.07 (0.62)
Subtype	(0.98)	(0.89)

Note: Correlations tested by Pearson's Correlation Coefficient

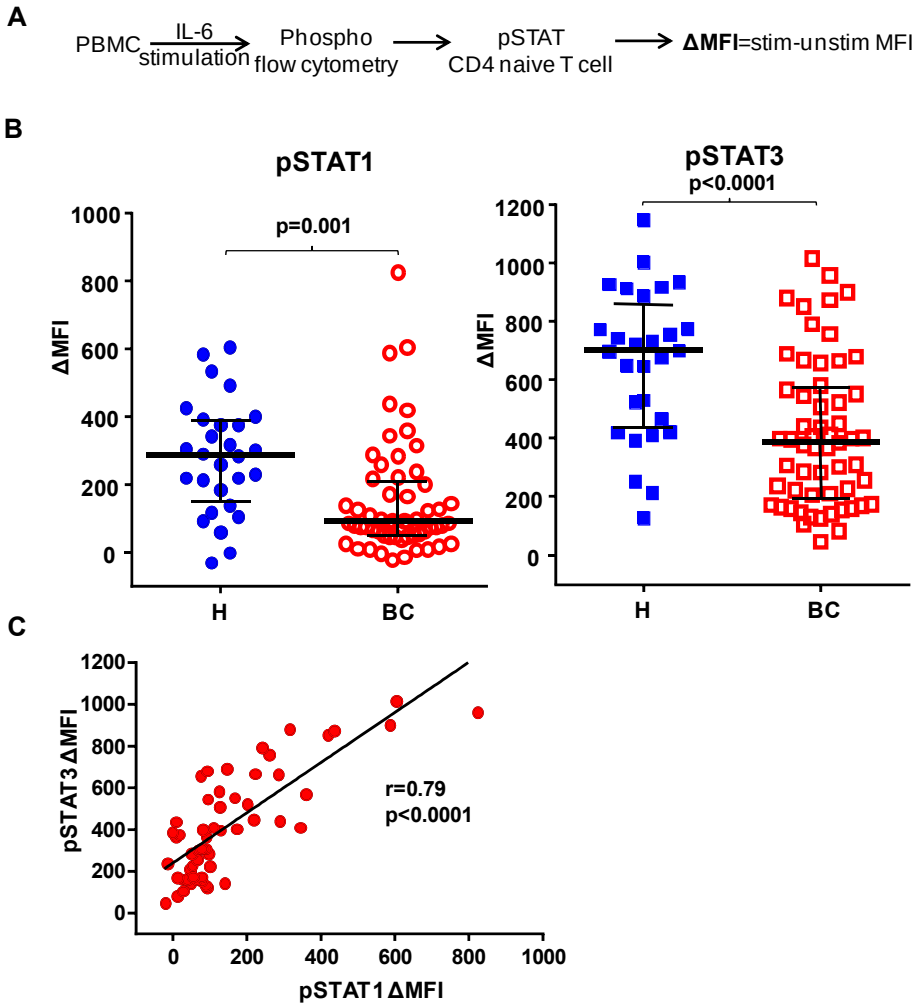

Figure 10. IL-6 signaling response is impaired in peripheral $CD4^+$ naïve T cells from BC patients. (A) Schematic representation of the experimental overview. Peripheral blood mononuclear cells (PBMCs) obtained from BC patients (BC) and healthy donors (H) were stimulated with 100 ng/ml of IL-6 for 15mins. IL-6 induced phosphorylation of STAT1 and STAT3 (pSTATs) in $CD4^+$ naïve T cells ($CD3^+CD4^+CD45RA^+$) were determined by phosphoflow cytometry with anti-pSTAT1 (pY701) and anti-pSTAT3 (pY705) antibodies. IL-6 signaling response was represented by ΔMFI (medium fluorescence intensity) which is the IL-6 stimulated MFI minus unstimulated MFI of pSTAT1 or pSTAT3. Blood from BC patients were from individuals who had been clinically followed for at least 12 months. (B) IL-6 induced phosphorylation of STAT1 ($p=0.001$) and STAT3 ($p<0.0001$) in peripheral $CD4^+$ naïve T cells were compared between BC patients (n=57, median age 51, range 27-85) and age-matched healthy donors (n=28, median age 53, range 18-72). Unpaired t-test. (C) The association between IL-6 induced pSTAT1 and pSTAT3 in $CD4^+$ naïve T cells from BC patients were determined by Pearson's correlation coefficient test ($r=0.79$, $p<0.0001$).

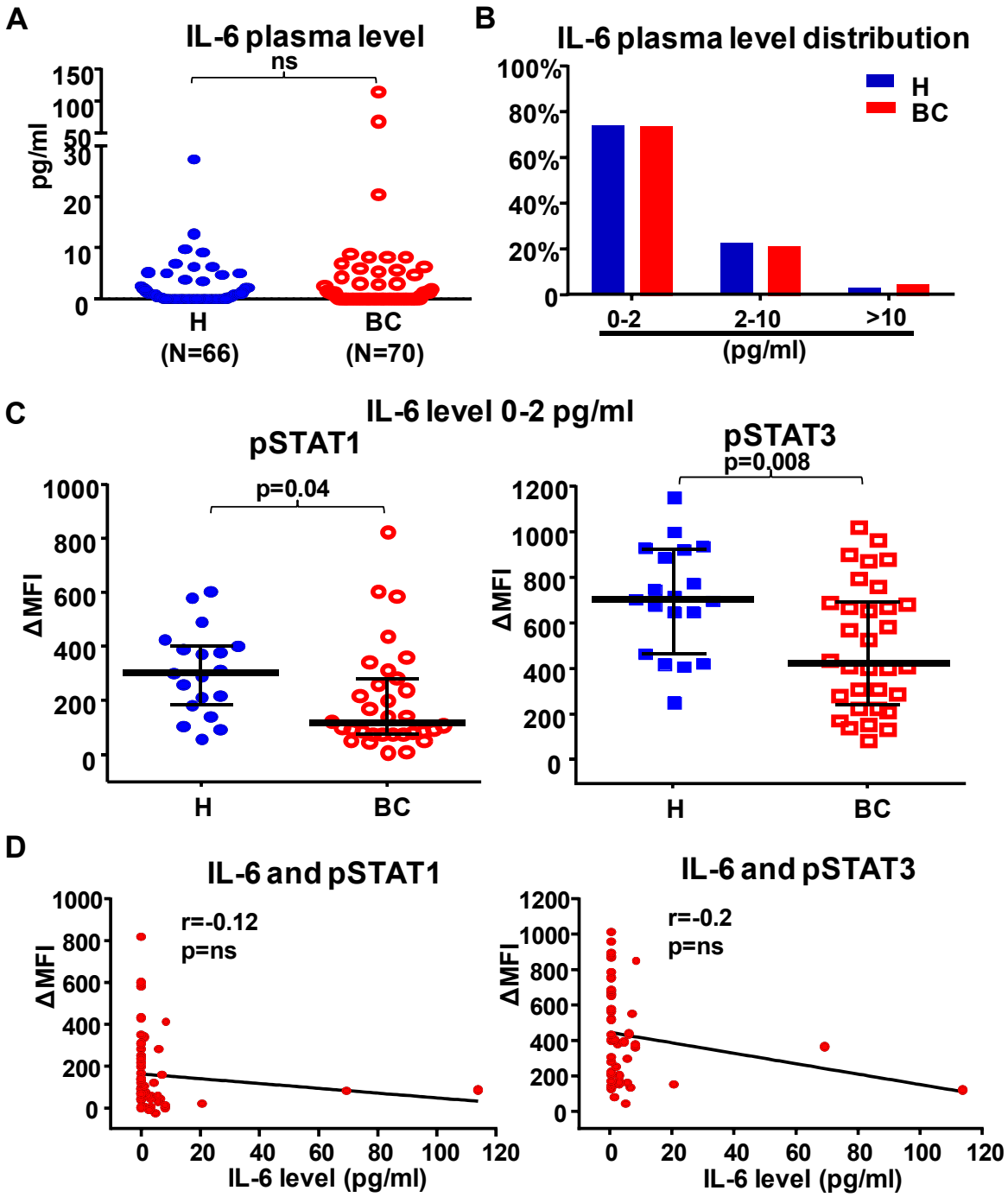

Figure 11. Impaired IL-6 signaling response is not caused by elevated IL-6 plasma levels. (A) IL-6 plasma levels in healthy donors (mean 2.0 pg/ml, median 0.25pg/ml) and BC patients (mean 4.2pg/ml, median 0 pg/ml) were determined by ELISA. Age-matched healthy donors (n=66, median age, range) to BC patients (n=70, median age, range). All the plasma from BC patients was collected at diagnosis prior to surgery or any therapy. (B) Distribution of IL-6 plasma levels over 0-2pg/ml, 2-10pg/ml and >10pg/ml in the healthy donors and BC patients. (C) Among the healthy donors and BC patients with normal IL-6 plasma level (0-2pg/ml), IL-6 induced phosphorylation of STAT1 (p=0.04) and STAT3 (p=0.008) in peripheral $CD4^+$ naïve T cells were compared. Unpaired t test. (D) The association between IL-6 plasma level and IL-6 induced pSTAT1 and pSTAT3 in $CD4^+$ naïve T cells from the BC patients were determined by Pearson's correlation coefficient test. (E) The surface expression levels of IL-6Rα and GP130 (p=0.03) on CD4 naïve T cells from healthy donors (n=25) and BC patients (n=31) were determined by flow cytometry with anti-IL-6Rα and anti-GP130 antibodies. Unpaired t-test. ns = not significant.

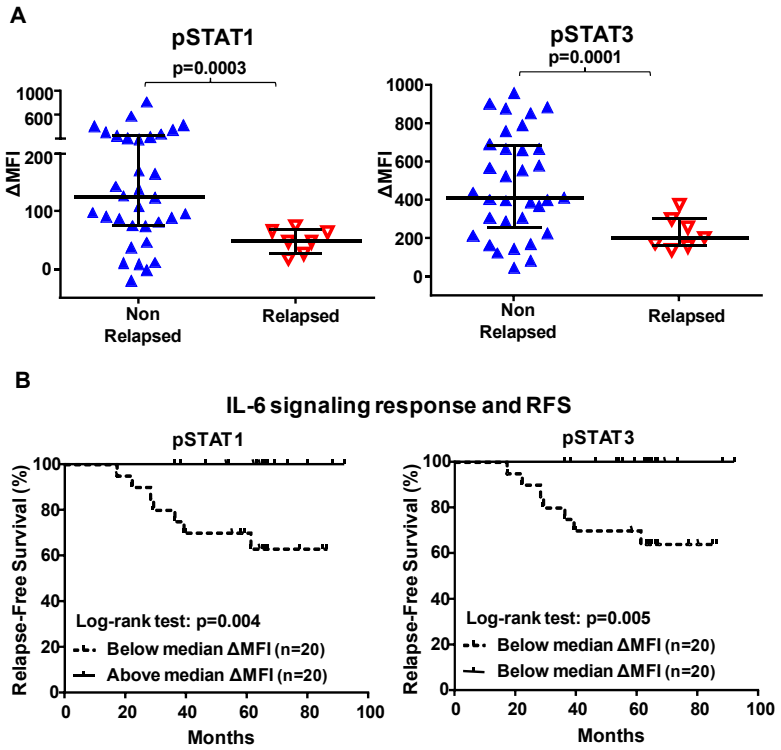

Figure 12. IL-6 signaling response has prognostic value for BC clinical outcome. (A) IL-6 induced phosphorylation of STAT1 (p=0.0003) and STAT3 (p=0.0001) in peripheral $CD4^+$ naïve T cells were compared between non-relapsed and relapsed BC patients. Blood from BC patients were collected at diagnosis prior to surgery or any therapy the patients have been clinically followed for at least 36 months. (B) Kaplan-Meier survival analysis was performed to evaluate the difference of relapse-free survival (RFS) between BC patients with lower and higher IL-6 signaling response (pSTAT1 p=0.004, pSTAT3 p=0.005). The median IL-6 induced phosphorylation of STAT1 or STAT3 (ΔMFI) was used as the cut-off to divide BC patients into lower and higher IL-6 signaling response groups.

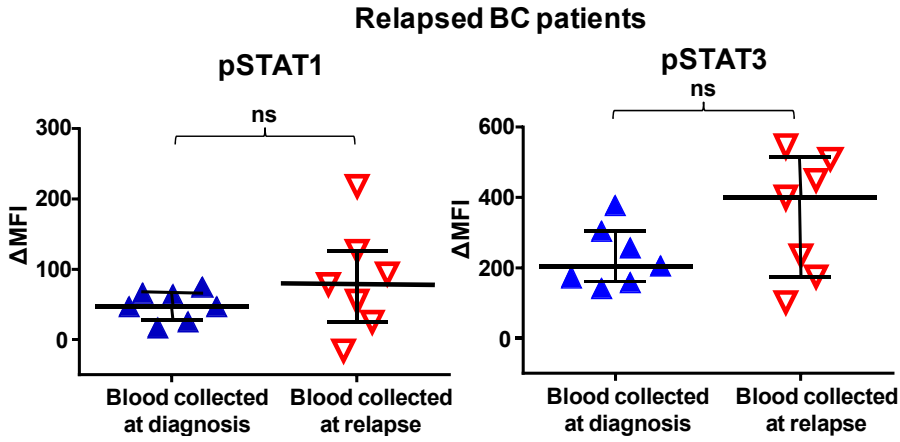

Figure 13. Impaired IL-6 signaling response is prolonged during BC progression. Among the relapsed BC patients, IL-6 induced phosphorylation of STAT1 and STAT3 in CD4 naïve T cells were compared between patients with blood collected at diagnosis (n=7) and patients with blood collected at relapse (n=7). Unpaired t-test. ns = not significant.

Aim 3. Select optimal integrated immunotherapy combinations in animals for clinical development.

Task 5. Select Optimal Integrated Immunotherapy Combinations in Animal Models for Clinical Development: months 12-60.

While some combinations of FDA approved cytokine therapeutics for cancer (IL-2 and IFN-α2b) have shown modest incremental efficacy, they have been limited by substantial toxicities (*34*). Previous cytokines tested clinically as cancer therapeutics were selected based on putative effects to enhance immune function rather than specifically to correct immune signaling defects in cancer. In addition, DC vaccination effectiveness may be hampered by an immunosuppressive environment, which prevents maturation and clustering in lymph nodes. Each of the key phases of the immune response—induction, amplification, and effector immune cell generation—is defective in breast cancer patients, so it follows that integrated immunotherapy combinations that address all of the phases of the normal immune response will be much more effective than individual treatments that address only one mechanism.

Developing integrated immunotherapeutic regimens to target the immune signaling defects that occur in each phase of the immune response (**Figure 14**), in combination with optimal DC-vaccination strategies using immunologically validated antigens, will generate highly functional and prolonged anti-tumor immune responses in breast cancer patients that will prevent recurrence and metastasis.

We will focus on developing a thorough approach to best take our findings about the 3D tumor microenvironment and its unique setting with our knowledge of cytokine signaling functions in immune and cancer cells and then attempt to assess *in vivo* effectiveness of combining the regimens for induction of optimal anti-tumor immunity. Then we will determine the optimal time to administer these regimens during disease progression, with and without chemotherapy. As surgery removes the primary tumor burden, we will focus our studies on the post-surgical setting where we envision immunotherapy is most effective to eradicate micrometastases to prevent relapse.

Task 5a. Optimize post-surgical murine model of breast cancer metastasis (month 12-36).

Task 5b. DC vaccination optimization by restoration of DC clustering and maturation (months 24-48).

Task 5c. Optimization of the amplification and effector phases by correcting chronic IL6-mediated defective T cell responses . (month 24-48).

Task 5d. Testing other strategies and combinations. (month 48-60).

Modulation of P2X4/P2X7/Pannexin-1 sensitivity to extracellular ATP via ivermectin induces a non-apoptotic and inflammatory form of cancer cell death

High extracellular adenosine triphosphate (ATP) is one of the major characteristics of the tumor microenvironment(*35, 36*). Exogenous ATP controls cellular and tissue defense/repair processes via signaling through P1, P2X, and P2Y purinergic receptors. P2X7 signaling has been associated with tumor growth and metastasis(*37-41*). High extracellular ATP levels also occur *in vivo* at sites of trauma, ischemia, or stroke and are associated with massive inflammatory responses and cell death (e.g. in excitable cells such as neurons). Thus, ATP can function as a prototypical danger signal that activates a potent immune response, but can also promote cancer progression. Considering these examples of diametrically opposed functions, ATP/purinergic signaling appears to play a complex role within the tumor microenvironment. Specifically, tumor growth and survival appears to critically depend on optimal extracellular ATP levels that balance tumor-promoting and

cytotoxic functions. As such, accumulation of extracellular ATP within the tumor microenvironment is tightly regulated and involves controlled release from the cancer cells as well as degradation by tumor-associated extracellular ATPases such as CD39 and CD73.

ATP associated cell death can involve a signaling pathway downstream of P2X7; its therapeutic potential has been demonstrated in multiple mouse models and clinical trials (*38*). However, the use of P2X7 agonists (ATP, ATPγS or Bz-ATP) is limited by systemic toxicity and fails to leverage elevated ATP concentrations found in the tumor microenvironment. In our effort to identify alternative approaches to target this pathway within the tumor microenvironment, we have been studying the commonly used anti-parasitic agent Ivermectin. The anti-tumor activity of both Ivermectin and structurally-related avermectins has been validated in xenogeneic(*42*) and immune-competent syngeneic mouse models(*43*); in addition, the agents demonstrated broad anti-cancer potential for various solid and hematological malignancies(*43*). To explain these activities, several mechanisms have been proposed. These include blockade of MDR exporters and enhanced uptake of doxorubicin/vincristine(*44, 45*); inactivation of PAK1 kinase(*46*); and suppression of the Wnt/β-catenin pathway(*47*). Importantly, avermectins have been shown to exert potent, anti-tumor effects *in vivo* at doses that were subtherapeutic *in vitro* (*43*). This implies that the compounds' actions may be potentiated by the tumor microenvironment and/or the immune system. Congruently, avermectins synergize with chemotherapeutic agents known to induce immunogenic cell death, such as doxorubicin; Ivermectin stimulates P2X4/P2X7/Pannexin-1 signaling, which augments inflammasome activation in myeloid cells(*48*).

Considering these findings, we hypothesized that purinergic signaling may be involved in the mechanism by which Ivermectin kills cancer cells or modulates the immune system. We found that Ivermectin kills mouse and human triple-negative breast cancer (TNBC) cells through augmented P2X7-dependent purinergic signaling associated with caspase-1 and caspase-3 activation. While caspase-3 activity is centrally involved in apoptotic cell death, previous reports indicate that Ivermectin kills leukemic cells in the context of cytosolic Cl^- influx and cell size increase; these features suggest another mode of cell death as apoptosis typically involves volume decreases. Since ATP plays a prominent role in regulating cell volume and promotes cancer cell death in response to hypotonic stress(*49*), we hypothesized that Ivermectin kills cancer cells in part by enhancing P2X7 sensitivity to ATP. In doing so, the compound appears to induce both an apoptotic and a non-apoptotic, inflammatory type of cell death. The ability of Ivermectin to induce an inflammatory and potentially immunogenic form of cell death is supported by 1) its ability to stimulate autophagy; and 2) recent data showing that ATP release from cancer cells undergoing ICD is mediated by the Ivermectin-sensitive P2X4/P2X7-gated Pannexin-1 channels(*50*). Below, we describe Ivermectin's killing of cancer cells through a mixed apoptotic and necrotic mode of cell death, the latter being most consistent with pyroptosis. Inflammatory and immunogenic forms of cell death are particularly important in the context of cancer types where tumor antigens and therapeutic targets are limited or unknown, such as TNBC, which was used as a model in our studies.

Ivermectin kills breast cancer cells through a mixed apoptotic and necrotic mechanism

Due to its ability to stimulate P2X4/P2X7/Pannexin-1 signaling in myeloid cells[14], we investigated Ivermectin as a prototype agent to modulate purinergic signaling in breast cancer cells. Mouse and human TNBC cells are sensitive to Ivermectin (**Figure 15A**), which exhibited IC50 values as low as 2 μM with extended exposure time (**Figure 15B**). Consistent with previous findings in leukemia, breast cancer cells manifested higher sensitivity than normal cells to Ivermectin (**Figure 15C**). More than 90% of dying cancer cells became directly necrotic (7AAD-positive). The remainder went through an Annnexin V/phosphatidylserine (PS) single positive apoptotic phase that quickly progressed to secondary necrosis (**Figure 15D and E**). Necrosis appears predominant during the first 4h of treatment, at which point the slower progressing apoptosis gains prominence. The pan-caspase inhibitor Z-vad-fmk inhibited cell death very effectively. The inhibitors of caspase-1 (VX-765), necroptosis (Necrostatin), and autosis (Digoxin) also demonstrated some protection (**Figure 15F**). We then investigated the downstream mediators of cell death. Cancer cells were treated with Ivermectin and analyzed for 1) PARP cleavage; 2) activation of caspase-1-a characteristic feature of the pyroptotic cell death pathway; and 3) caspase-3 activity typically observed in

classical apoptosis. Ivermectin treatment results in rapid cleavage of PARP that occurs in the context of potent caspase-1 and caspase-3 activation (**Figure 15G**). Interestingly, western blot analysis shows that caspase-1 is constitutively activated/cleaved in the breast cancer cells (**Figure 15H**), consistent with reports showing constitutive activation of the inflammasome in human melanoma (*51*). Our flow data based on fluorescently labeled capspase-1 substrate-specific probe, however, suggest the existence of multiple levels of regulation of caspase-1 activity that can be further enhanced by Ivermectin.Our findings indicate that Ivermectin may kill cancer cells though a mechanism combining apoptosis and necrosis/pyroptosis.

As described in previous reports, Ivermectin may increase cell volume, affect cytosolic Ca^{2+} flux, and increase production of ROS in leukemic cells(*42*). Since maintenance of cell volume is regulated by ATP-, Ca^{2+}- and ROS-dependent mechanisms, we decided to investigate their potential involvement in Ivermectin-induced cell death. Our findings suggest that it is not the magnitude of Ivermectin-induced ROS that kills cancer cells. Unlike ROS of mitochondrial origin, NADPH oxidases-generated ROS are known to play important signaling roles and some NADPH oxidases are also Ca^{2+}-dependent. We demonstrated that Ivermectin-induced ROS are regulated partially by Ca^{2+}, NADPH oxidases, ATP and P2X7 (**Figure 16A**). Of note, an inhibitor of NADPH oxidases, DPI, (rather than ROS scavengers) is able to transiently block Ivermectin-induced killing (**Figure 16B**). Short-term exposure to DPI and high doses of Ivermectin were found to be most informative since NADPH oxidases are essential for tumor cell growth and prolonged exposure to DPI exacerbates oxidative stress and becomes directly toxic. These data imply that Ca^{2+}/NADPH/ROS signaling is directly involved in the mechanism of killing. Importantly, Ivermectin was found to be synergistic with irradiation, H_2O_2-generated ROS, and chemotherapeutic agents that are known inducers of ROS stress such as doxorubicin and paclitaxel (**Figure 16C**). This is consistent, with previous data in leukemia showing synergy between Ivermectin and the ROS-inducing chemotherapeutic drugs doxorubicin and cytarabine(*42*). Although NADPH oxidases-generated ROS can contribute to ROS imbalance and ROS-mediated killing, the magnitude of Ivermectin-induced ROS does not appear to be directly cytotoxic.

Dual roles of ATP and purinergic signaling in Ivermectin's killing

Ivermectin has been shown to enhance P2X4-dependent purinergic signaling in myeloid cells, driving a ROS-dependent pathway that normally activates the cytosolic NLRP3 inflammasome(*48, 52-56*). Since volume control depends on ATP release and Ca^{2+} signaling, we investigated the role of ATP and purinergic signaling in Ivermectin-induced killing. Ivermectin killing was initially enhanced by both depleting extracellular ATP with Apyrase (**Figure 17A**) and blocking purinergic signaling with a non-specific inhibitor of P2 receptors (Suramin) (Figure S3A). We also showed that extracellular Ca^{2+} and ATP prevent Ivermectin-induced cell swelling, which provides a mechanistic explanation for their initial protective role (**Figure 17B**). We decided to investigate whether the sustained increase in cytosolic Ca^{2+} levels described earlier was preceded by extracellular ATP release from non-necrotic viable cells. ATP release from the P2X4/P2X7-gated Pannexin-1 channels is a potent feed-forward mechanism operating in autophagic cancer cells and activated leukocytes. Ivermectin synergized with ATP in opening P2X4/P2X7/Pannexin-1 channels resulting in partial permeabilization of the plasma membrane of 4T1.2 cells to YOPRO-1 without compromising cell viability (**Figure 17C**). Analysis of supernatants from TNBC cells demonstrated an immediate increase in extracellular ATP levels in response to Ivermectin, followed by a period of its transient depletion (**Figure 17D**). Using cells engineered to express a membrane-bound form of Luciferase, similar results were obtained by measuring plasma membrane-proximal extracellular ATP levels (**Figure 17E**). These findings suggest that ATP release is necessary to balance an increased demand/consumption of extracellular ATP. A significant body of literature indicates that cancer cells are sensitive to high concentrations of extracellular ATP (*35, 37*). Ivermectin can enhance signaling of the P2X4 receptor, which can complex with both pannexin-1 and death-mediating P2X7 receptors (*57, 58*). Therefore, we hypothesized that Ivermectin may modulate the sensitivity of cancer cells to ATP. We demonstrated a dramatic up-regulation of P2X7 and Ivermectin-sensitive P2X4 receptors in 4T1.2 cells (**Figure 17F**). We found that the semi-specific P2X7 inhibitor KN-62 was effective at blocking Ivermectin-induced necrotic and apoptotic cell death (**Figure 17G**).

Excessive CaMKII signaling and MPTP contribute to cell death

KN-62 is not completely specific for the P2X7 receptor and also weakly inhibits Ca^{2+}/Calmodulin-dependent protein kinase II (CaMKII). More than 1 μM of KN-62 is needed to protect against Ivermectin-induced cell death; and this value is consistent with KN-62's inhibition of CAMKII. CaMKII activity correlates with sustained increase in cytosolic Ca^{2+} (**Figure 18A**) and is known to be a downstream target of P2X7 receptor signaling and to mediate neuronal cytotoxicity in the context of I/R, stroke and neurodegenerative diseases, pathologic conditions where ATP-mediated excitotoxicity is known to play a prominent role(*59, 60*). We investigated whether Ivermectin-induced cell death was mediated by P2X7, CaMKII, or a combination of both. To this end, we used a CaMKII-specific inhibitor (KN-93) while knocking down the P2X7 receptor with shRNA. KN-93 effectively blocked Ivermectin-induced cell death, confirming that over-activation of the CaMKII underlies the initial wave of cell death in many Ivermectin-sensitive cancer cell lines (**Figure 18B**). We also demonstrated that while lower doses of Ivermectin cause mitochondrial hyperpolarization, massive cancer cell death occurs in the context of a sudden depolarization of mitochondria (**Figure 18C**) and that blockade of mitochondrial permeability transition pore (MPTP), the downstream effector of this cell death pathway, is able to confer partial protection against Ivermectin (**Figure 18D**).

CaMKII-independent P2X7-mediated killing

Given the low affinity of P2X7 for ATP, high extracellular ATP concentrations are needed for P2X7 receptors to deliver death signals. As extracellular ATP is transiently depleted and protective during Ivermectin-induced cell death, we sought to clarify the way in which the P2X7 pathway is activated and involved in cytotoxicity. To this end, we compared the ability of Ivermectin to kill wild type and P2X7-knockdown 4T1.2 cells (**Figure 19A**). Overall, P2X7 knockdown cells were more resistant to ATP and ATP/Ivermectin cytotoxicity (**Figure 19B**), which is consistent with a pivotal role for the P2X7 receptor in ATP-mediated cytotoxicty. In addition, the P2X7 knockdowns were more resistant to ATP- and ATP/Ivermectin-induced membrane permeabilization to YOPRO-1 (**Figure 19C**), suggesting that over-activation of this protective mechanism might lead to cytotoxicity. High concentrations of extracellular ATP kill cancer cells in a P2X7-dependent fashion but with much slower kinetics compared to Ivermectin. Therefore, in addition to targeting ATP/P2X4/P2X7 signaling, the drug likely affects other pathways. We show that Ivermectin and ATP can synergistically kill even ATP- and Ivermectin-resistant human cancer cell lines (**Figure 19D**). We further compared the ability of CaMKII/MPTP and P2X7 inhibition to provide short-term (4h) versus long-term (24h) protection against Ivermectin. While inhibition of NADPH, CaMKII, and MPTP provided significant protection against Ivermectin cytotoxicity within the first 4h, only KN-62 was able to provide long-term protection against Ivermectin and ATP that extended up to 24h (**Figure 19E**). Thus the balance between the apoptotic and necrotic death pathways downstream of the P2X7 receptor appears to be regulated by the complex interplay between extracellular ATP, ROS levels, and CaMKII activation.

Ivermectin induces autophagy

The mixed apoptotic and necrotic mechanism of killing prompted us to analyze Ivermectin's ability to modulate some features previously associated with immunogenic cell death: HMGB1/ATP release and the surface exposure of Calreticulin (CRT). Release of ATP and surface exposure of CRT on apoptotic cells have already been linked to autophagy and ER stress (*50, 61, 62*). We demonstrate that Ivermectin is a potent inducer of autophagy (**Figure 20A-B**), consistent with its ability to stimulate ATP release and P2X4/P2X7/Pannexin-1 membrane permeabilization. Moreover, while Ivermectin does not significantly impact surface CRT (**Figure 20C**, bottom panel), its ability to up-regulate plasma membrane exposure of mannose-6-phosphate (M6P) receptors could potentially render cancer cells susceptible to bystander CTL/NK cell-mediated killing, as described recently (**Figure 20C**, top panel)(*63, 64*). Ivermectin also appears to be a potent inducer of HMGB1 release (**Figure 20D**), preceding that of LDH (**Figure 20E**), consistent with both necrosis and reports describing the key role of caspase-1 in regulating non-classical secretion of HMGB1 (*65, 66*).

Synergistic effects of Doxorubicin and Ivermectin *in vivo*

Recent clinical data has revealed the potential of checkpoint blockade (CTLA4, PD-1) to unleash potent immune responses in melanoma and lung cancer patients, with a subset of them achieving complete and durable remissions. Responsiveness to checkpoint blockade also appears to correlate with tumor immunogenicity/mutational load. This raises the question of whether checkpoint blockade would be a suitable strategy in less/poorly immunogenic types of cancer, such as breast cancer. In these settings a combination of checkpoint blockade and cancer vaccination seems to be the most appropriate. To that end, we have decided to investigate the potential of synergistic drug combinations to induce immunogenic cell death. Preliminary in vitro data identified the anti-parasitic drug Ivermectin as an inducer of a particularly inflammatory and non-apoptotic form of cell death through modulation of the P2X4/P2X7/Pannexin-1 channels and enhanced sensitivity of breast cancer cells to extracellular ATP. We also found that Ivermectin is synergistic with Doxorubicin, a standard of care chemotherapeutic agent that is known to induce autophagy, ATP release, and immunogenic cell death. We decided to investigate whether Doxorubicin and Ivermectin would demonstrate similar synergy in vivo using the murine 4T1.2 model, a well established model of triple-negative breast cancer. Treatments were initiated at day 4 after tumor challenge when tumor size reached approximately 5 mm in diameter, as treating bigger tumors at later time points was ineffective. We show that Doxorubicin (5 mg/kg) and Ivermectin (5 mg/kg) alone have detectable but limited activity against 4T1.2 cells. The combination of Doxorubicin and Ivermectin demonstrates superior protection validating our in vitro synergy data and confirming the existence of a meaningful therapeutic window (**Figure 21**). The 5 mg/kg dose of Ivermectin appears to be safe as extended 3 week daily treatments didn't cause lethality but also didn't provide further tumor protection. Paradoxically, oral delivery of Ivermectin was optimal as direct intra-tumoral injection of Ivermectin was counterproductive and actually failed to protect (**Figure 22**). Ivermectin doses of 10 mg/kg could be tolerated only for up to several days and in combination with Doxorubicin resulted in shrinking of large established 4T1.2 tumors but mice succumbed to synergistic toxicity (data not shown), defining the therapeutic limitations of this combination and encouraging the search of other even more potent Ivermectin-based synergistic drug combinations.

Plans for the next 12 months:

- Evaluate other potential Ivermectin-based synergistic drug combinations based on our preliminary *in vitro* studies, including Rapamycin and proteasome inhibitors.
- Evaluate the ability of Ivermectin to induce immunogenic cell death in the 4T1.2 triple-negative breast cancer model, alone or in combination with Doxorubicin. Parallel studies will be performed in an Ova-expressing breast cancer model in order to study the effect of our drug combination on anti-tumor antigen-specific responses.

- Studies will also be extended to include other types of breast cancer including Her-2-or ER-positive tumor models.

- Investigate the effect of adding PD-1 checkpoint blockade, with the hope that further potentiation of the anti-tumor immune responses induced by the Dox-IVM combo might result in durable and curative responses.

Supporting Data/Figures:

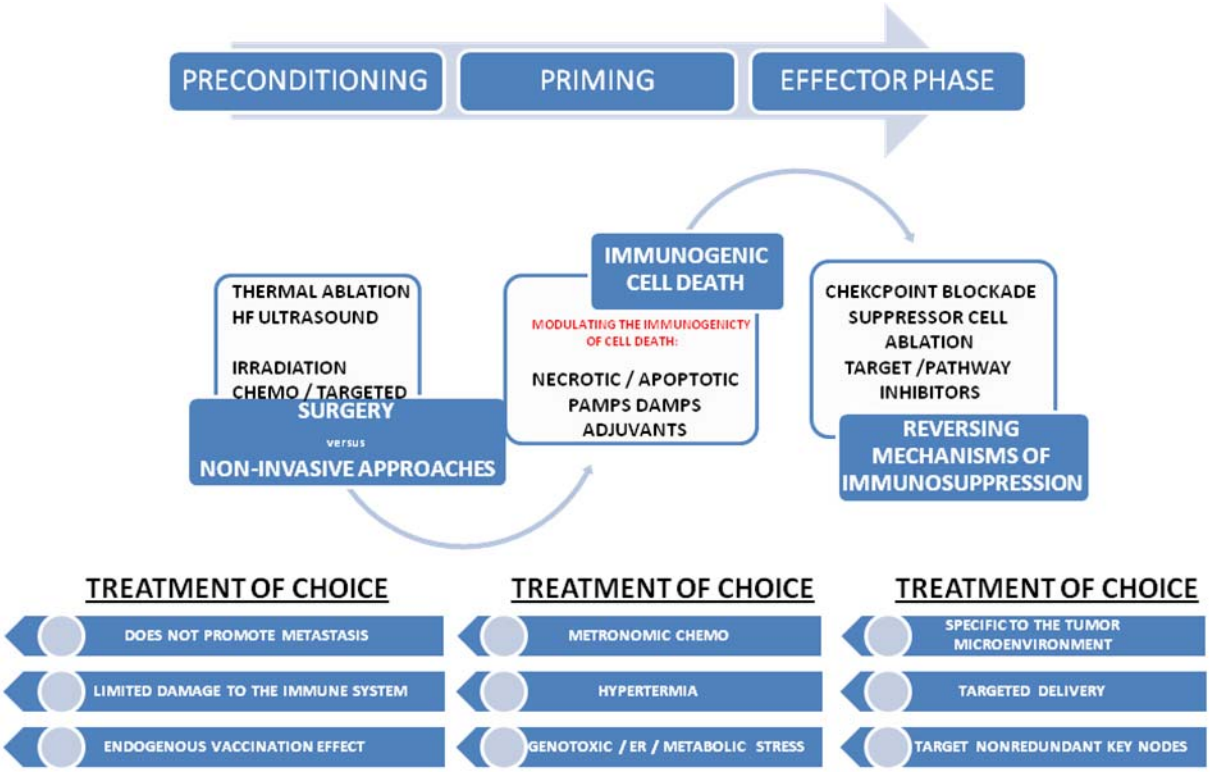

Figure 14. Experimental Design. Illustration of the steps involved in genomic profiling of cancer cells and CAS to identify differential gene expression patterns in the reconstructed co-cultured cancer cell and stromal cell 3D organoids.

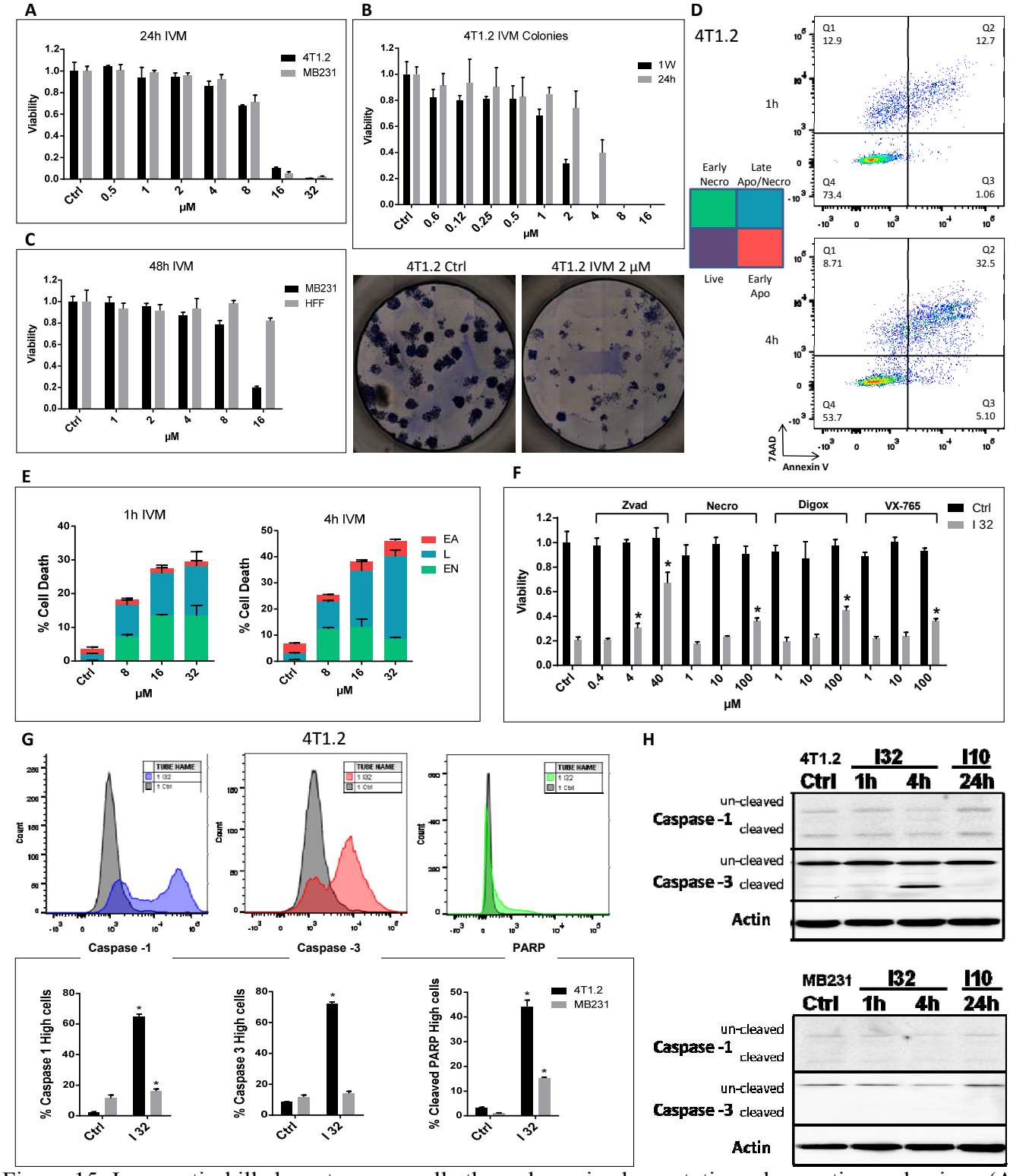

Figure 15. Ivermectin kills breast cancer cells through a mixed apoptotic and necrotic mechanism. (A) Mouse (4T1.2) and human (MDA-MB-231) TNBC cells manifest similar sensitivity to Ivermectin. Viability of cells treated with various doses of Ivermectin for 24h. (B) Extended exposure time reduces IC50 values to as low as 2 μM. 4T1.2 cells were seeded at 100 cells/well and individual colonies were counted after a week. Cancer cells were exposed to Ivermectin during the initial 24h or during the entire duration of the assay. (C) MDA-MB-231 breast cancer cells manifest higher sensitivity to Ivermectin compared to normal non-transformed human foreskin fibroblasts (HFFs). (D) Flow cytometry analysis showing that cell death proceeds through two distinct pathways: a directly necrotic 7AAD-single positive or Annexin V/PS-single positive apoptotic pathway. (E) Kinetics of necrotic versus apoptotic killing of 4T1.2 breast cancer cells. (F) Ivermectin-induced cell death can be reversed by inhibition of various controlled cell death pathways. 4T1.2 cells were treated for 4h with 32 μM

Ivermectin in the presence of µM concentrations of Z-vad-fmk, Necrostatin-1, Digoxin, or VX-765, as indicated. (G) Activation of Caspase-1, Caspase-3 and cleavage of PARP in 4T1.2 and MDA-MB-231 cells treated with 32 µM for 4h. Asterisk (*) indicates $p<0.05$ relative to untreated or Ivermectin alone controls, respectively. (H) Western blot analysis showing constitutive and Ivermectin-induced cleavage of Caspases 1 and 3 in murine (top) and human (bottom) breast cancer cells.

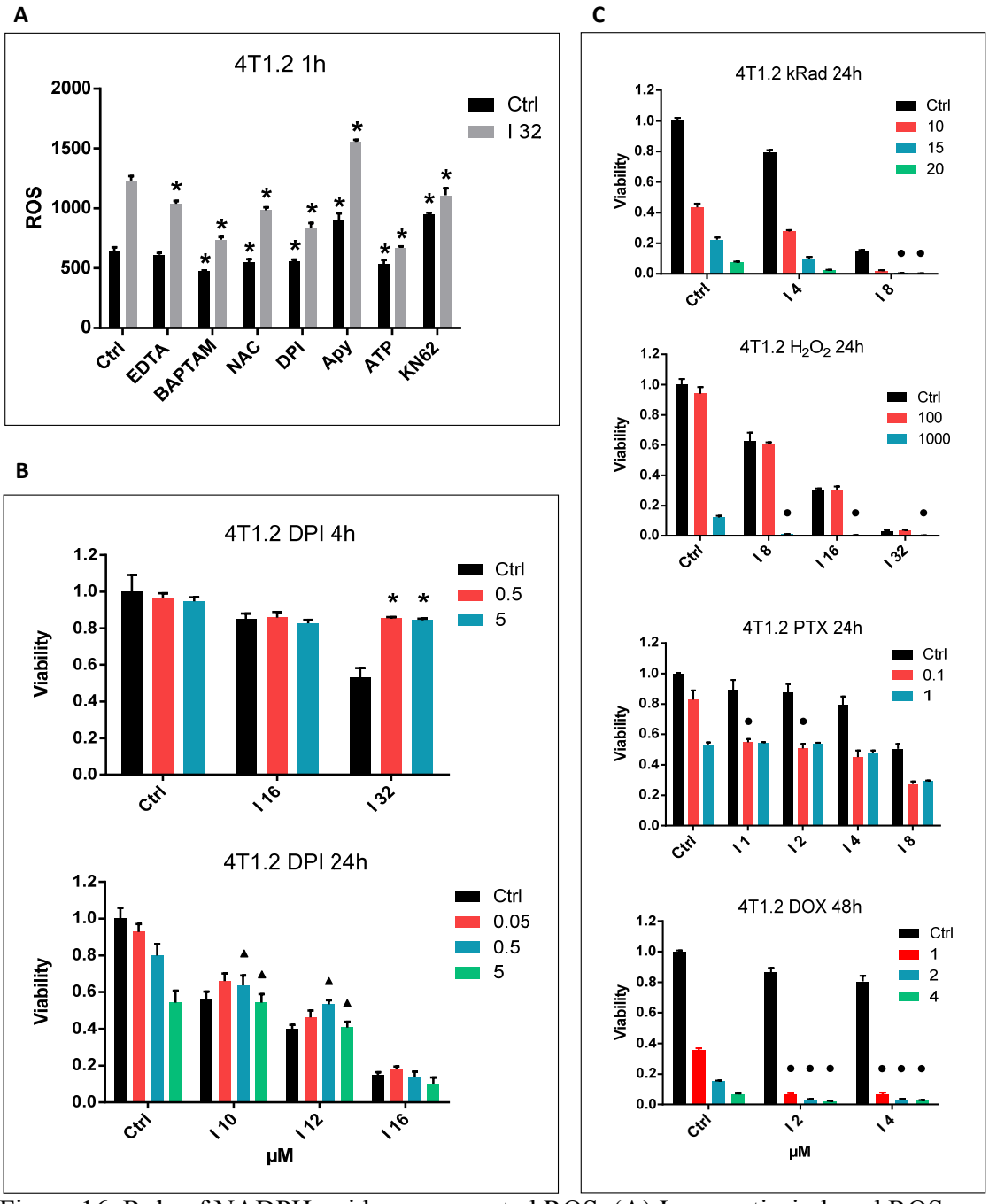

Figure 16. Role of NADPH oxidases-generated ROS. (A) Ivermectin-induced ROS are Ca^{2+} -, ATP-, and P2X7-regulated. 4T1.2 cells were labeled with a ROS detection probe and treated for 1h with 32 µM Ivermectin in the presence of 1 mM EDTA, 5mM NAC, 5 µM DPI, 2500 µunits/ml Apyrase, 3 mM ATP, and 10 µM KN-62. (B) Ivermectin-induced cell death is transiently reversed by inhibition of NADPH oxidases with DPI (µM concentrations as indicated). Triangles (▲) indicate significant antagonism CI>1.0. (C) Synergy between Ivermectin and H_2O_2- or irradiation-generated ROS, as well as the ROS-inducing chemotherapeutic agents paclitaxel (PTX) and doxorubicin (DOX). 4T1.2 cancer cells were irradiated (10-20 kRad) or treated with H_2O_2 (10-1000 µM), PTX (0.1-1 µM), or DOX (1-4 µM) and incubated with Ivermectin for 24h/48h. Circles (●)

indicate significant synergy CI<1.0, see **Table 1**. Asterisk (*) indicates p<0.05 relative to untreated or Ivermectin alone controls, respectively.

Table 1.

CompuSyn CI values:
<0.8 synergistic
0.8-1.2 additive
>1.2 antagonistic

	I 4	I 8
kRad 10	1.34	1.03
kRad 15	1.16	0.75
kRad 20	0.94	0.63

	I 8	I 16	I 32
H_2O_2 10	0.98	1.17	1.05
H_2O_2 100	1.46	1.39	1.05
H_2O_2 1000	0.24	0.20	0.18

	I 2	I 4
Dox 1	0.43	0.61
Dox 2	0.42	0.56
Dox 4	0.49	0.71

	I 1	I 2	I 4	I 8
PLT 0.1	0.35	0.52	0.84	1.08
PLT 1	1.30	1.51	1.52	1.32

CompuSyn CI values:	<0.8 synergistic		0.8-1.2 additive	>1.2 antagonistic	
	I 4	**I 8**		**I 8**	**I 16**
kRad 15	1.16	0.75	**H_2O_2 100**	1.46	1.39
kRad 20	0.94	0.63	**H_2O_2 1000**	0.24	0.20
	I 1	**I 2**		**I 2**	**I 4**
PTX 0.1	0.35	0.52	**DOX 1**	0.43	0.61
PTX 1	1.30	1.51	**DOX 2**	0.42	0.56

CompuSyn CI values:	<0.8 synergistic			0.8-1.2 additive	>1.2 antagonistic	
	I 1	**I 2**	**I 4**	**I 8**	**I 16**	**I 32**
kRad 10			1.34	1.03		
kRad 15			1.16	0.75		
kRad 20			0.94	0.63		
H_2O_2 10				0.98	1.17	1.05
H_2O_2 100				1.46	1.39	1.05
H_2O_2 1000				0.24	0.20	0.18
PLT 0.1	0.35	0.52	0.84	1.08		
PLT 1	1.30	1.51	1.52	1.32		
Dox 1		0.43	0.61			
Dox 2		0.42	0.56			
Dox 4		0.49	0.71			

CompuSyn CI values:	<0.8 synergistic	0.8-1.2 additive	>1.2 antagonistic
	I 2	**I 4**	**I 8**
kRad 15		1.16	0.75
kRad 20		0.94	0.63
H_2O_2 1000			0.24
PLT 0.1	0.52	0.84	1.08
Dox 1	0.43	0.61	
Dox 2	0.42	0.56	
Dox 4	0.49	0.71	

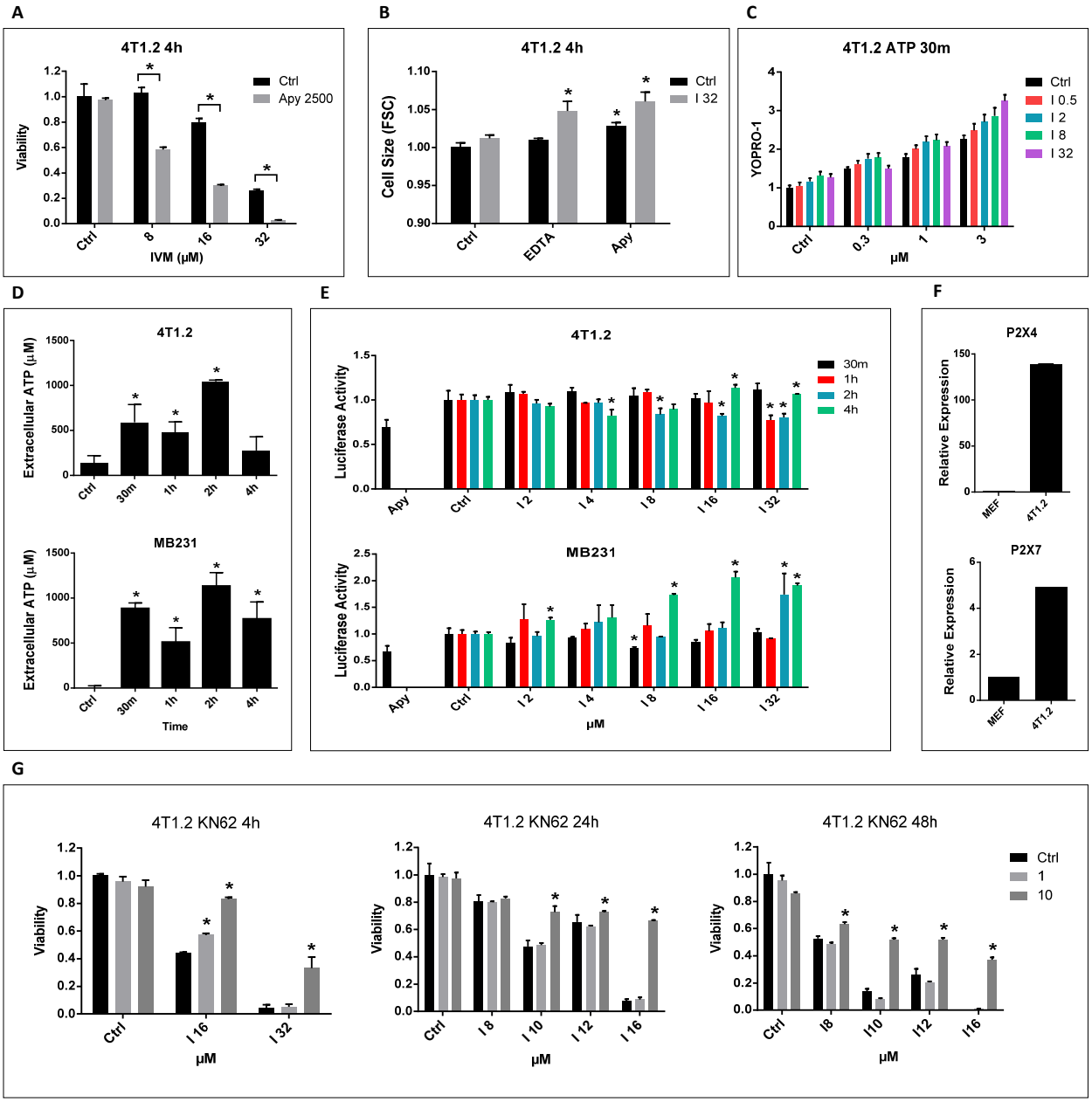

Figure 17. Dual roles of ATP and purinergic signaling in Ivermectin's killing. (A) Depletion of extracellular ATP with Apyrase (2500 μunits/ml) exacerbates killing of 4T1.2 cell by Ivermectin. (B) Extracellular Ca^{2+} and ATP contain Ivermectin-induced cell swelling. 4T1.2 cells were treated with 32 μM Ivermectin for 4h in the presence of 1 mM EDTA or 2500 μunits/ml Apyrase. (C) Ivermectin (0.5-32 μM**)** and high concentrations of extracellular ATP (0.3-3 mM) synergistically open pannexin-1 channels and permeabilize the membrane on live cells (7AAD-positive dead cells were gated out). 4T1.2 cells were treated for 30min as indicated in the presence of 7AAD and 5 μM YOPRO-1. (D) Analysis of supernatants from Ivermectin-treated murine and human TNBC cells showing rapid release of ATP followed by its transient depletion. Depletion of extracellular ATP with Apyrase (2500 μunits/ml) was used as a positive control. (E) Analysis of membrane-proximal ATP levels using cancer cells engineered to express a membrane-bound Luciferase. (F) qPCR demonstrating over-expression of P2X4 and P2X7 receptors in mouse 4T1.2 breast cancer cells versus mouse embryonic fibroblasts (MEF). (G) The P2X7-specific inhibitor KN-62 (1-10 μM) blocks Ivermectin cytotoxicity (IVM 8-32 μM, 4-48h treatments). Asterisk (*) indicates $p<0.05$ relative to untreated or Ivermectin alone controls, respectively.

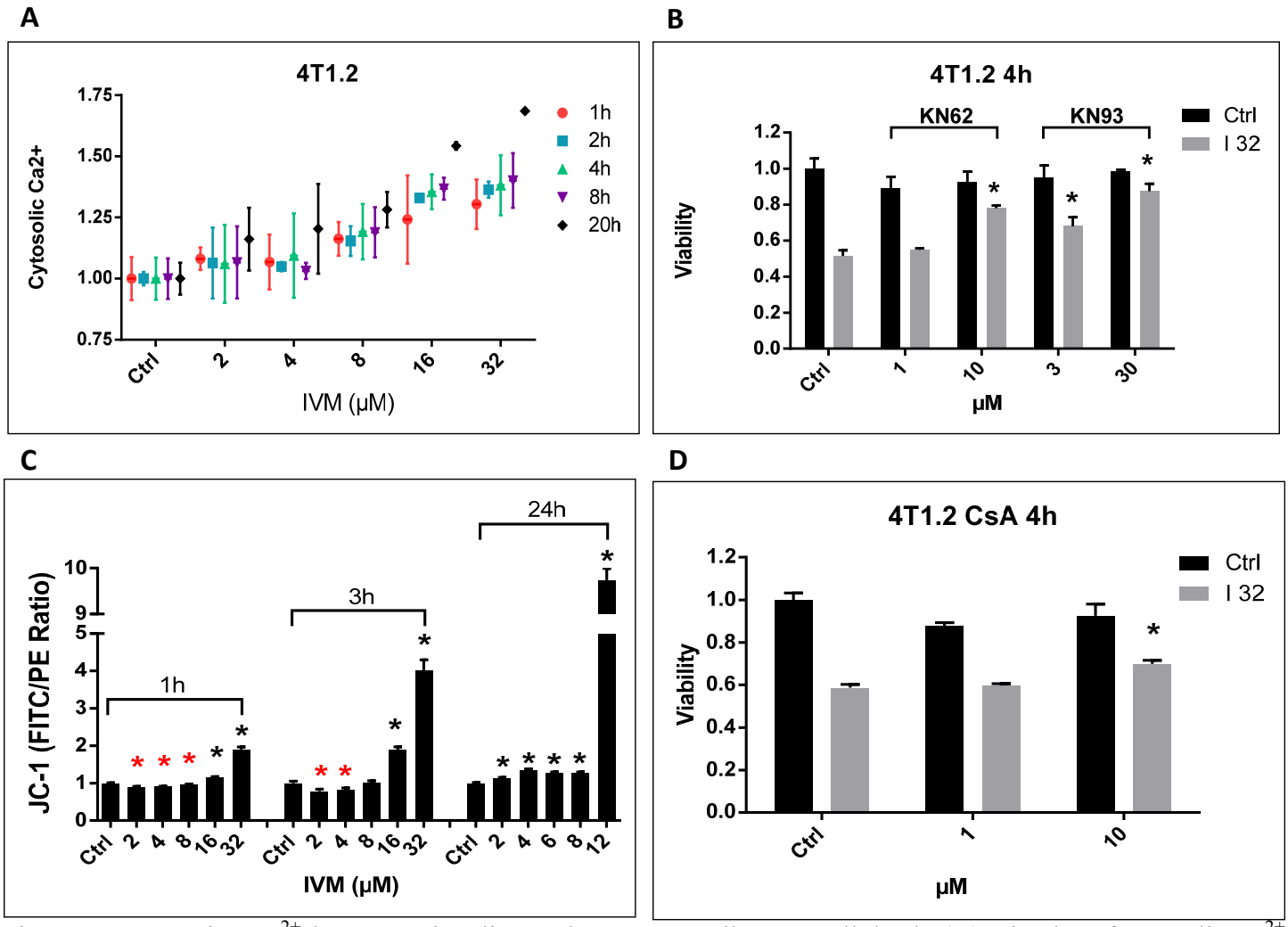

Figure 18. Excessive Ca^{2+} /CaMKII signaling and MPTP contribute to cell death. (A) Kinetics of cytosolic Ca^{2+} increase in 4T1.2 cells treated with Ivermectin. (B) Inhibition of CaMKII is equally effective at blocking the initial cytotoxicity of Ivermectin. 4T1.2 cells were treated for 4h with 32 μM Ivermectin in the presence of the P2X7/CaMKII dual inhibitor KN-62 or the CaMKII-specific inhibitor KN-63, at μM concentrations as indicated. (C) Flow cytometry analysis of JC-1 loaded 4T1.2 cells showing that high doses of Ivermectin result in a sudden mitochondrial de-polarization, while lower doses cause similar effects but after transient hyper-polarization. (D) MPTP contributes to Ivermectin. 4T1.2 cells were treated for 4h with 32 μM Ivermectin in the presence of the MPTP inhibitor Cyclosporin A at μM concentrations as indicated. Asterisk (*) indicates $p<0.05$ relative to untreated or Ivermectin alone controls, respectively.

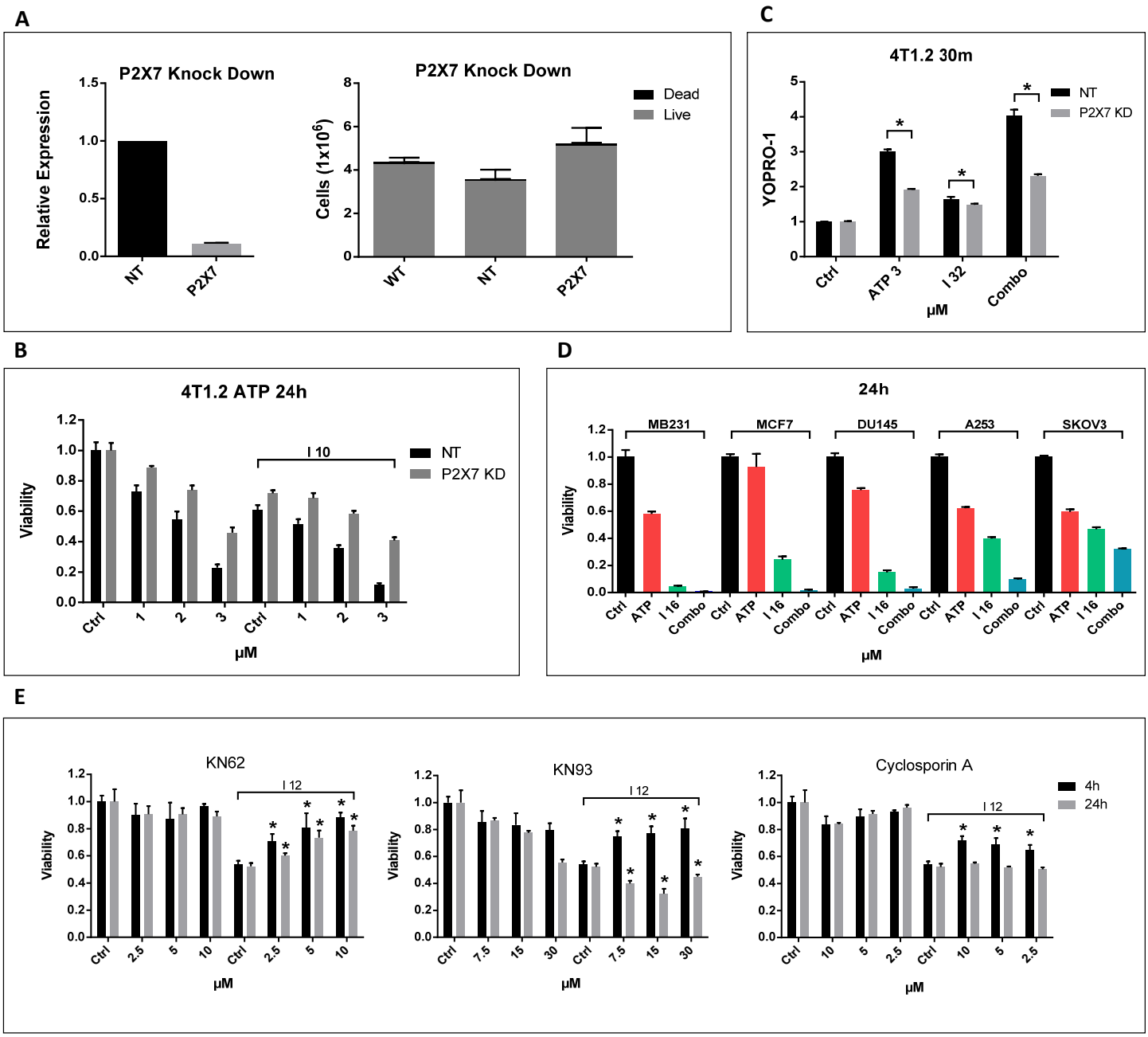

Figure 19. CaMKII-independent P2X7-mediated killing**.** (A) qPCR showing the extent of gene knockdown in 4T1.2 cells transfected with shRNA targeting the P2X7 receptor versus non-targeting (NT) control (left panel). The right panel shows that P2X7 knockdown does not compromise tumor cell growth and viability. One million wt, shRNA(NT) and shRNA(P2X7) 4T1.2 cells were plated and incubated for 48h before evaluation of cell numbers and viability. (B) P2X7 knockdown cells are more resistant to ATP and the ATP/IVM combo. 4T1.2 cells were treated for 24h with 1-3 mM ATP, 6-10 µM Ivermectin, or combinations of ATP and Ivermectin. P2X7 knockdown suppresses the synergy between Ivermectin and high dose ATP, as shown by calculation of combination index (CI) values, see **Table 2**. (C) P2X7 knockdown cells are resistant to ATP/Ivermectin induced membrane permeabilization (Asterisk (*) indicates $p<0.05$). (D) The combination of Ivermectin (16 µM) and exogenous ATP (3 mM) can synergistically kill even some resistant human cancer cell lines like breast (MCF7), prostate (DU-145), head and neck (A253), and ovarian (SKOV3) cancer cells. (E) Comparison of the protective effects of P2X7, CaMKII, and NADPH oxidases inhibition in short-term (4h, 32 µM IVM) and long-term (24h, 12 µM IVM) exposure of 4T1.2 cells to Ivermectin. Asterisk (*) indicates $p<0.05$ relative to Ivermectin alone controls.

Table 2.

CI values:	<0.8 Synerg	0.8-1.2 Addit	>1.2 Antag
4T1.2 shRNA (P2X7)			
	I 6	I 8	I 10
ATP 1	1.49	1.39	1.35
ATP 2	1.18	1.03	1.11
ATP 3	0.96	0.91	0.89
4T1.2 shRNA (NT)			
ATP 1	1.18	1.01	1.24
ATP 2	1.17	1.01	1.10
ATP 3	0.67	0.64	0.63

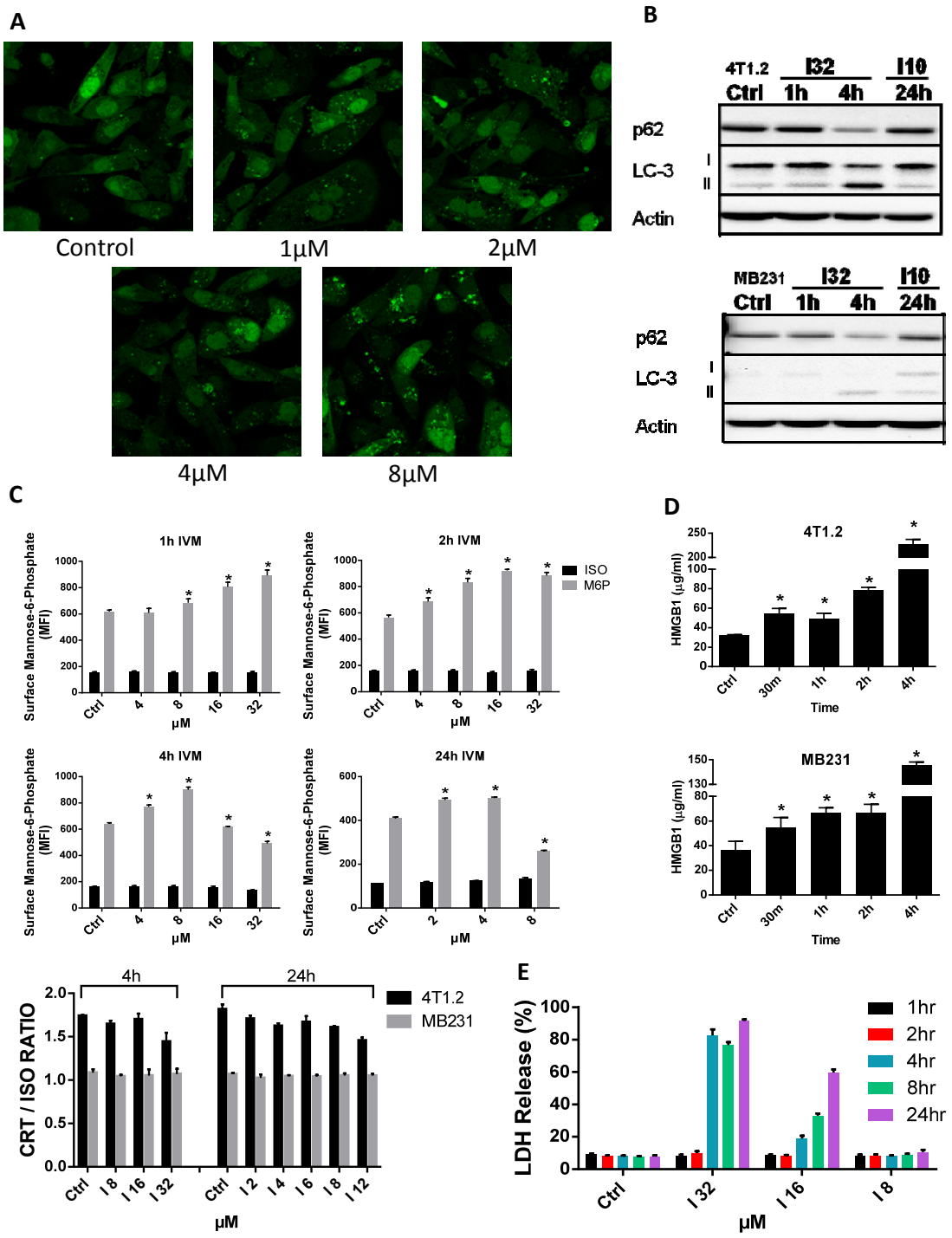

Figure 20. Ivermectin induces autophagy. (A) Ivermectin induces autophagy in breast cancer cells. MDA-MB-231 GFL-LC3 cells were treated with different doses of Ivermectin for 24h and formation of green fluorescent puncta was evaluated by confocal fluorescence microscopy. (B) Western blot confirming the induction of autophagy in both murine and human breast cancer cells, as evidenced by LC3 lipidation and autophagic degradation of p62(SQSTM1). (C) Ivermectin up-regulates surface exposure of M6P receptor (top panel) but does not impact the exposure of Calreticulin (CRT) (bottom panel). MDA-MB-231 cells (triplicates) were treated with different doses of Ivermectin for up to 24h and surface stained with antibody-specific for the human M6P receptor versus isotype control. Similarly, 4T1.2 and MB231 cells were treated with different doses of Ivermectin for 4-24h, and were stained with an antibody specific for both human and mouse CRT versus isotype control. Mean fluorescent intensity (MFI) values and ratios versus isotype control were calculated after gating on live/membrane-intact cells. (D) Ivermectin (32 μM) induces release of HMGB1 from murine and human TNBC cells (triplicates). (E) Ivermectin treatment induces release of cytosolic LDH, data are normalized

to maximum release (lysis). Asterisk (*) indicates $p<0.05$ relative to untreated or Ivermectin alone controls, respectively.

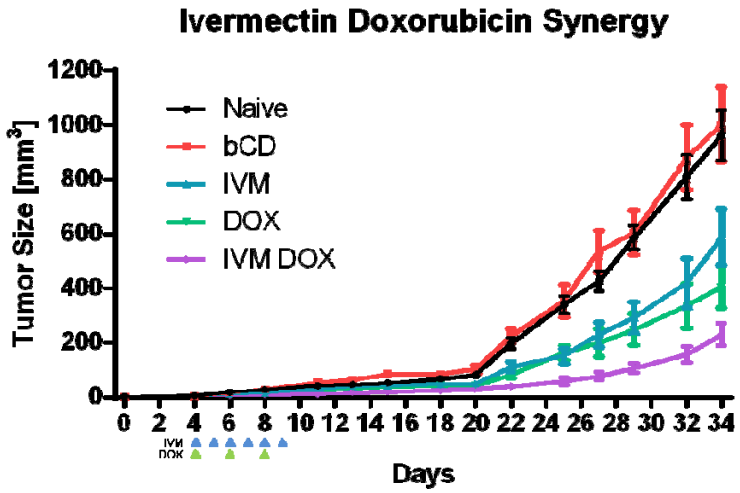

Figure 21. Ivermectin and Doxorubicin have synergistic effect in the 4T1.2 breast cancer model. Balb/c mice were orthotopically injected with 100,000 4T1.2 cells in the mammary gland. Starting at day 4 after tumor challenge, mice were treated with 5 mg/kg daily Ivermectin (IVM) administered orally and 5 mg/kg Doxorubicin (Dox) administered intra-peritoneally every other day for a total of 6 and 3 treatments, respectively. Mice were given IVM alone, DOX alone, or the combination of both drugs without any significant treatment-associated toxicity. Tumor growth was measured with caliper three times weekly, and was followed until the naïve (untreated) or beta-cyclodextran (bCD) vehicle control mice succumbed to disease. Tumor volume was calculated using the $V = (W(2) \times L)/2$ formula. Error bars represent SEM based on 12 animals per treatment group.

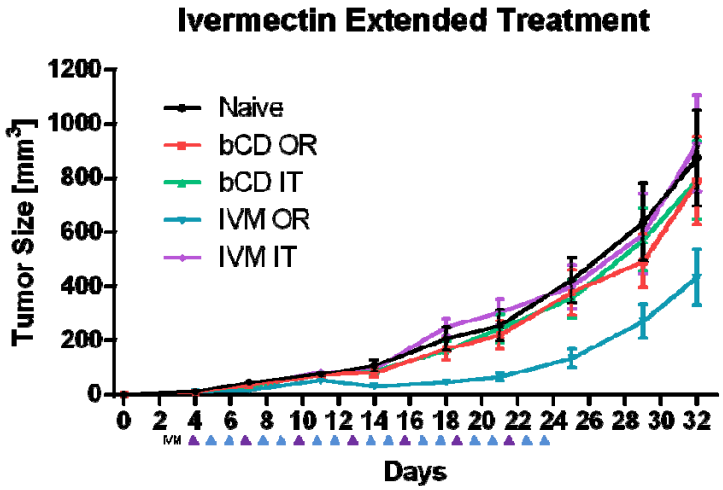

Figure 22. Extended oral treatments with Ivermectin are effective and safe but do not provide further improvement in protection against the 4T1.2 breast tumors. Balb/c mice were orthotopically injected with 100,000 4T1.2 cells in the mammary gland. Starting at day 4 after tumor challenge, mice were treated with 5 mg/kg daily Ivermectin (IVM) administered orally (OR) versus beta-cyclodextran (bCD) vehicle control, for up to 3 weeks. A group of mice received direct intra-tumoral injection (IT) of IVM every third day, which was given instead of their daily oral treatments. Tumor growth was measured with caliper two times weekly, and was followed until the naïve (untreated) or beta-cyclodextran (bCD) vehicle control mice succumbed to disease. Tumor volume was calculated using the $V = (W(2) \times L)/2$ formula. Error bars represent SEM based on 8 animals per treatment group.

KEY RESEARCH ACCOMPLISHMENTS:

- Substantial progress has been made in successfully characterizing and growing breast cancer patient-specific cancer cells, MSCs, and CAS (from both primary and metastatic tumors), and using these cells to generate 3D organoids.

- Demonstrated that *in vivo* injection of suspended E007 alone or in combination with MSCs in C57BL/6 mouse created tumors from injection into the mammary fat pad.

- Generated 3-D CAF aggregates mixed with human breast cancer cells in order to recapitulate human breast tumor tissue microenvironment and this technique will be further utilized for implantation of mouse-based 3-D E007+MSC aggregates into B6 tumor recipient animals.

- Determined that IL-6 signaling responses are dysfunctional in an expanded cohort of breast cancer patients versus age-matched healthy donors.

- Established that IL-6 signaling defects in $CD4^+$ naïve T cells were not due to elevated IL-6 levels in the plasma of breast cancer patients.
- Generated data which suggests that IL-6 signaling responsiveness in peripheral $CD4^+$ naïve T cells could be used to predict the clinical outcome of BC patients.

- Identified Ivermectin as a prototype agent to allosterically modulate P2X4 receptors can switch the balance between the dual pro-survival and cytotoxic functions of purinergic signaling in breast cancer cells which is mediated through augmented opening of the P2X4/P2X7-gated Pannexin-1 channels that drives a mixed apoptotic and necrotic mode of cell death associated with activation of caspase-1 and is consistent with pyroptosis.

- Demonstrated that cancer cell death is dependent on ATP release and death signals downstream of P2X7 receptors that can be reversed by inhibition of NADPH oxidases-generated ROS, Ca^{2+}/Calmodulin-dependent protein kinase II (CaMKII) or mitochondrial permeability transition pore (MPTP).

- Ivermectin induces autophagy and release of ATP and HMGB1, key mediators of inflammation and inflammation-induced pathology that have also been associated with immunogenic cell death.

- Demonstrated synergistic effects using the combination of Ivermectin and Doxorubicin *in vivo*.

- Determined that extended oral treatments with Ivermectin are effective and safe but do not provide further improvement in protection against the 4T1.2 breast tumors.

.

REPORTABLE OUTCOMES: Provide a list of reportable outcomes that have resulted from this research to include:

- Modulation of P2X4/P2X7/Pannexin-1 sensitivity to extracellular ATP via ivermectin induces a non-apoptotic and inflammatory form of cancer cell death. - submitted
- IL-6 signaling responses predict clinical outcome in breast cancer patients – in preparation

CONCLUSION:

We have a strong research team for this project, which includes assistant research professor Dr. Brile Chung, PhD postdoctoral fellow Dr. Dobrin Draganov, research associates Gayathri Srinivasan and Gilbert Acosta. We have worked closely with the CoH IACUC office on animal protocols and two have been approved. We continue to develop an in-depth understanding of the immune system within the setting of the tumor microenvironment. We have made progress in developing methods to better analyze the relationships between primary tumor and metastatic growths with their surrounding microenvironment and implications for immune response and dendritic cell function *in vitro* using 3D microculture techniques. We have further investigated and tested alternative methods of combinatorial drugs in attempts to eradicate cancer cells while preserving the immune system. We are well positioned to gain further insights in the next 12 months that will aid in our goal of restoring long term immune function in breast cancer patients to optimal levels, and subsequently eradicate metastases to prevent relapse in breast cancer patients.

APPENDICES:

None at this time.

PERSONNEL:

Peter P. Lee, MD – PI	25% Effort
Brile Chung, PhD – Assistant Research Professor	100% Effort
Dobrin Draganov, PhD – Post Doctoral Fellow	100% Effort
Gayathri Srinivasan, Research Associate I	100% Effort
Gilbert Acosta, Research Associate I	100% Effort

REFERENCES:

1. C. N. Baxevanis *et al.*, Tumor specific cytolysis by tumor infiltrating lymphocytes in breast cancer. *Cancer* **74**, 1275 (Aug 15, 1994).
2. G. B. Cannon, R. Pomerantz, Cell-mediated immune responses--prognostic indicators of survival from breast cancer. *Int J Cancer* **44**, 995 (Dec 15, 1989).
3. J. L. McCoy, R. Rucker, J. A. Petros, Cell-mediated immunity to tumor-associated antigens is a better predictor of survival in early stage breast cancer than stage, grade or lymph node status. *Breast Cancer Res Treat* **60**, 227 (Apr, 2000).
4. H. E. Kohrt *et al.*, Profile of immune cells in axillary lymph nodes predicts disease-free survival in breast cancer. *PLoS Med* **2**, e284 (Sep, 2005).
5. B. Weigelt, A. T. Lo, C. C. Park, J. W. Gray, M. J. Bissell, HER2 signaling pathway activation and response of breast cancer cells to HER2-targeting agents is dependent strongly on the 3D microenvironment. *Breast Cancer Res Treat* **122**, 35 (Jul, 2010).
6. M. Vanneman, G. Dranoff, Combining immunotherapy and targeted therapies in cancer treatment. *Nature reviews. Cancer* **12**, 237 (Apr, 2012).
7. B. Ljujic *et al.*, Human mesenchymal stem cells creating an immunosuppressive environment and promote breast cancer in mice. *Scientific reports* **3**, 2298 (Jul 29, 2013).
8. T. D. Tlsty, L. M. Coussens, Tumor stroma and regulation of cancer development. *Annual review of pathology* **1**, 119 (2006).
9. A. V. Meleshina *et al.*, Influence of mesenchymal stem cells on metastasis development in mice in vivo. *Stem cell research & therapy* **6**, 15 (2015).
10. Y. Jung *et al.*, Recruitment of mesenchymal stem cells into prostate tumours promotes metastasis. *Nature communications* **4**, 1795 (2013).
11. N. S. Zuckerman, Y. Noam, A. J. Goldsmith, P. P. Lee, A self-directed method for cell-type identification and separation of gene expression microarrays. *PLoS computational biology* **9**, e1003189 (Aug, 2013).
12. P. C. Heinrich, I. Behrmann, G. Muller-Newen, F. Schaper, L. Graeve, Interleukin-6-type cytokine signalling through the gp130/Jak/STAT pathway. *The Biochemical journal* **334 (Pt 2)**, 297 (Sep 1, 1998).
13. H. Korkaya, S. Liu, M. S. Wicha, Regulation of Cancer Stem Cells by Cytokine Networks: Attacking Cancers Inflammatory Roots. *Clin Cancer Res*, (Jun 17, 2011).
14. H. Knupfer, R. Preiss, Significance of interleukin-6 (IL-6) in breast cancer (review). *Breast Cancer Res Treat* **102**, 129 (Apr, 2007).
15. R. Salgado *et al.*, Circulating interleukin-6 predicts survival in patients with metastatic breast cancer. *Int J Cancer* **103**, 642 (Feb 20, 2003).
16. A. Kimura, T. Kishimoto, IL-6: regulator of Treg/Th17 balance. *Eur J Immunol* **40**, 1830 (Jul, 2010).
17. X. Zhang, T. Goel, L. L. Goodfield, S. J. Muse, E. T. Harvill, Decreased leukocyte accumulation and delayed Bordetella pertussis clearance in IL-6-/- mice. *J Immunol* **186**, 4895 (Apr 15, 2011).
18. M. Kopf *et al.*, Impaired immune and acute-phase responses in interleukin-6-deficient mice. *Nature* **368**, 339 (Mar 24, 1994).
19. S. Pflanz *et al.*, WSX-1 and glycoprotein 130 constitute a signal-transducing receptor for IL-27. *J Immunol* **172**, 2225 (Feb 15, 2004).
20. E. Tassi *et al.*, Non-redundant role for IL-12 and IL-27 in modulating Th2 polarization of carcinoembryonic antigen specific CD4 T cells from pancreatic cancer patients. *PloS one* **4**, e7234 (2009).
21. T. Yoshimoto, K. Yasuda, J. Mizuguchi, K. Nakanishi, IL-27 suppresses Th2 cell development and Th2 cytokines production from polarized Th2 cells: a novel therapeutic way for Th2-mediated allergic inflammation. *J Immunol* **179**, 4415 (Oct 1, 2007).
22. S. Pflanz *et al.*, IL-27, a heterodimeric cytokine composed of EBI3 and p28 protein, induces proliferation of naive CD4(+) T cells. *Immunity* **16**, 779 (Jun, 2002).

23. N. Morishima *et al.*, A pivotal role for interleukin-27 in CD8+ T cell functions and generation of cytotoxic T lymphocytes. *J Biomed Biotechnol* **2010**, 605483 (2010).
24. N. Morishima *et al.*, Augmentation of effector CD8+ T cell generation with enhanced granzyme B expression by IL-27. *J Immunol* **175**, 1686 (Aug 1, 2005).
25. K. P. Strauss, Implementing the telecommunications provisions. *Milbank Q* **69 Suppl 1-2**, 238 (1991).
26. G. Regis, S. Pensa, D. Boselli, F. Novelli, V. Poli, Ups and downs: the STAT1:STAT3 seesaw of Interferon and gp130 receptor signalling. *Semin Cell Dev Biol* **19**, 351 (Aug, 2008).
27. L. Y. Kong *et al.*, A novel phosphorylated STAT3 inhibitor enhances T cell cytotoxicity against melanoma through inhibition of regulatory T cells. *Cancer Immunol Immunother* **58**, 1023 (Jul, 2009).
28. M. Kortylewski *et al.*, Inhibiting Stat3 signaling in the hematopoietic system elicits multicomponent antitumor immunity. *Nat Med* **11**, 1314 (Dec, 2005).
29. R. J. Critchley-Thorne *et al.*, Impaired interferon signaling is a common immune defect in human cancer. *Proceedings of the National Academy of Sciences of the United States of America* **106**, 9010 (Jun 2, 2009).
30. L. Avalle, S. Pensa, G. Regis, F. Novelli, V. Poli, STAT1 and STAT3 in tumorigenesis: A matter of balance. *JAKSTAT* **1**, 65 (Apr 1, 2012).
31. T. Bachelot *et al.*, Prognostic value of serum levels of interleukin 6 and of serum and plasma levels of vascular endothelial growth factor in hormone-refractory metastatic breast cancer patients. *Br J Cancer* **88**, 1721 (Jun 2, 2003).
32. P. M. Ridker, N. Rifai, M. J. Stampfer, C. H. Hennekens, Plasma concentration of interleukin-6 and the risk of future myocardial infarction among apparently healthy men. *Circulation* **101**, 1767 (Apr 18, 2000).
33. E. A. Rakha, Pitfalls in outcome prediction of breast cancer. *Journal of clinical pathology* **66**, 458 (Jun, 2013).
34. L. Anasagasti-Angulo, Y. Garcia-Vega, S. Barcelona-Perez, P. Lopez-Saura, I. Bello-Rivero, Treatment of advanced, recurrent, resistant to previous treatments basal and squamous cell skin carcinomas with a synergistic formulation of interferons. Open, prospective study. *BMC Cancer* **9**, 262 (2009).
35. G. Burnstock, F. Di Virgilio, Purinergic signalling and cancer. *Purinergic signalling* **9**, 491 (Dec, 2013).
36. P. Pellegatti *et al.*, Increased level of extracellular ATP at tumor sites: in vivo imaging with plasma membrane luciferase. *PloS one* **3**, e2599 (2008).
37. G. Burnstock, A. Verkhratsky, Long-term (trophic) purinergic signalling: purinoceptors control cell proliferation, differentiation and death. *Cell death & disease* **1**, e9 (2010).
38. N. White, G. Burnstock, P2 receptors and cancer. *Trends in pharmacological sciences* **27**, 211 (Apr, 2006).
39. C. J. Dixon *et al.*, Extracellular nucleotides stimulate proliferation in MCF-7 breast cancer cells via P2-purinoceptors. *British journal of cancer* **75**, 34 (1997).
40. E. Adinolfi *et al.*, P2X(7) receptor: Death or life? *Purinergic signalling* **1**, 219 (Sep, 2005).
41. E. Adinolfi *et al.*, Expression of P2X7 receptor increases in vivo tumor growth. *Cancer research* **72**, 2957 (Jun 15, 2012).
42. S. Sharmeen *et al.*, The antiparasitic agent ivermectin induces chloride-dependent membrane hyperpolarization and cell death in leukemia cells. *Blood* **116**, 3593 (Nov 4, 2010).
43. V. A. Drinyaev *et al.*, Antitumor effect of avermectins. *European journal of pharmacology* **501**, 19 (Oct 6, 2004).
44. S. Furusawa *et al.*, Potentiation of Doxorubicin-Induced Apoptosis of Resistant Mouse Leukaemia Cells by Ivermectin. *Pharmacy and Pharmacology Communications* **6**, 129 (2000).
45. Y. N. Korystov *et al.*, Avermectins inhibit multidrug resistance of tumor cells. *European journal of pharmacology* **493**, 57 (Jun 16, 2004).
46. H. Hashimoto, S. M. Messerli, T. Sudo, H. Maruta, Ivermectin inactivates the kinase PAK1 and blocks the PAK1-dependent growth of human ovarian cancer and NF2 tumor cell lines. *Drug discoveries & therapeutics* **3**, 243 (Dec, 2009).
47. A. Melotti *et al.*, The river blindness drug Ivermectin and related macrocyclic lactones inhibit WNT-TCF pathway responses in human cancer. *EMBO molecular medicine* **6**, 1263 (Oct, 2014).

48. M. Seil *et al.*, Ivermectin-dependent release of IL-1beta in response to ATP by peritoneal macrophages from P2X(7)-KO mice. *Purinergic signalling* **6**, 405 (Dec, 2010).
49. N. Selzner *et al.*, Water induces autocrine stimulation of tumor cell killing through ATP release and P2 receptor binding. *Cell death and differentiation* **11 Suppl 2**, S172 (Dec, 2004).
50. I. Martins *et al.*, Molecular mechanisms of ATP secretion during immunogenic cell death. *Cell death and differentiation* **21**, 79 (Jan, 2014).
51. M. Okamoto *et al.*, Constitutively active inflammasome in human melanoma cells mediating autoinflammation via caspase-1 processing and secretion of interleukin-1beta. *The Journal of biological chemistry* **285**, 6477 (Feb 26, 2010).
52. M. Seil, M. El Ouaaliti, J. P. Dehaye, Secretion of IL-1beta triggered by dynasore in murine peritoneal macrophages. *Innate immunity* **18**, 241 (Apr, 2012).
53. A. Kawano *et al.*, Involvement of P2X4 receptor in P2X7 receptor-dependent cell death of mouse macrophages. *Biochemical and biophysical research communications* **419**, 374 (Mar 9, 2012).
54. A. Kawano *et al.*, Regulation of P2X7-dependent inflammatory functions by P2X4 receptor in mouse macrophages. *Biochemical and biophysical research communications* **420**, 102 (Mar 30, 2012).
55. H. Sakaki *et al.*, P2X4 receptor regulates P2X7 receptor-dependent IL-1beta and IL-18 release in mouse bone marrow-derived dendritic cells. *Biochemical and biophysical research communications* **432**, 406 (Mar 15, 2013).
56. S. C. Hung *et al.*, P2X4 assembles with P2X7 and pannexin-1 in gingival epithelial cells and modulates ATP-induced reactive oxygen species production and inflammasome activation. *PloS one* **8**, e70210 (2013).
57. P. Pelegrin, A. Surprenant, Pannexin-1 mediates large pore formation and interleukin-1beta release by the ATP-gated P2X7 receptor. *The EMBO journal* **25**, 5071 (Nov 1, 2006).
58. S. Locovei, E. Scemes, F. Qiu, D. C. Spray, G. Dahl, Pannexin1 is part of the pore forming unit of the P2X(7) receptor death complex. *FEBS letters* **581**, 483 (Feb 6, 2007).
59. D. Leon, C. Hervas, M. T. Miras-Portugal, P2Y1 and P2X7 receptors induce calcium/calmodulin-dependent protein kinase II phosphorylation in cerebellar granule neurons. *The European journal of neuroscience* **23**, 2999 (Jun, 2006).
60. R. Gomez-Villafuertes *et al.*, Ca2+/calmodulin-dependent kinase II signalling cascade mediates P2X7 receptor-dependent inhibition of neuritogenesis in neuroblastoma cells. *The FEBS journal* **276**, 5307 (Sep, 2009).
61. G. Kroemer, L. Galluzzi, O. Kepp, L. Zitvogel, Immunogenic cell death in cancer therapy. *Annual review of immunology* **31**, 51 (2013).
62. A. Q. Sukkurwala *et al.*, Immunogenic calreticulin exposure occurs through a phylogenetically conserved stress pathway involving the chemokine CXCL8. *Cell death and differentiation* **21**, 59 (Jan, 2014).
63. S. Kim *et al.*, Radiation-induced autophagy potentiates immunotherapy of cancer via up-regulation of mannose 6-phosphate receptor on tumor cells in mice. *Cancer immunology, immunotherapy : CII* **63**, 1009 (Oct, 2014).
64. R. Ramakrishnan, D. I. Gabrilovich, The role of mannose-6-phosphate receptor and autophagy in influencing the outcome of combination therapy. *Autophagy* **9**, 615 (Apr, 2013).
65. L. Vande Walle, T. D. Kanneganti, M. Lamkanfi, HMGB1 release by inflammasomes. *Virulence* **2**, 162 (Mar-Apr, 2011).
66. B. Lu, H. Wang, U. Andersson, K. J. Tracey, Regulation of HMGB1 release by inflammasomes. *Protein & cell* **4**, 163 (Mar, 2013).